ANALYSIS AND INTERPRETATION OF COMPRESSIONAL (P-WAVE) AND SHEAR (SH-WAVE) REFLECTION SEISMIC AND GEOLOGIC DATA OVER THE BANE DOME, GILES COUNTY, VIRGINIA

by

Mark J. Gresko

Dissertation submitted to the Faculty of the
Virginia Polytechnic Institute and State University
in partial fulfillment of the requirements for the degree of
Doctor of Philosophy
in
Geological Sciences

APPROVED:

J. K. Costain, Chairman

G. A. Bollinger

C. Coruh

L. Glover III

E. S. Robinson

J. A. Snoke

March 1, 1985

Blacksburg, Virginia

ANALYSIS AND INTERPRETATION OF COMPRESSIONAL (P-WAVE) AND SHEAR (SH-WAVE) REFLECTION SEISMIC AND GEOLOGIC DATA OVER THE BANE DOME, GILES COUNTY, VIRGINIA

by

Mark J. Gresko

J. K. Costain, Chairman

Geological Sciences

(ABSTRACT)

Approximately 37 km of predominantly 24-fold P-wave Vibroseis data and 16 km of 24-fold SH-wave Vibroseis data were acquired in the southern portion of the folded Appalachians near the Bane Dome in Giles County, Virginia. Data processing techniques included the application of newly developed methods for crossdip removal as well as the determination of statics solutions in the case of time variant shifts within the data traces. Minimum-phase filter deconvolution was also applied for the removal of reverberating energy and multiples recorded on the SH-wave lines. V_p/V_s ratios were used to aid in the determination of lithologies in the absence of bore-hole data.

Interpreted thickening of the Lower Cambrian to Upper Precambrian sequence beneath the Bane Dome appears to represent Eocambrian rifting. Faults generated at that time may now be reactivated by the present stress regime, causing earthquake activity in this area. Interpretation of the seismic data supports a duplex structure proposed for the Paleozoic rocks

of the Bane Dome Complex within the Narrows thrust sheet of southwestern Virginia.

ACKNOWLEDGEMENTS

Support for these ongoing seismic risk studies have been provided by the Nuclear Regulatory Commission. Support for the Virginia Tech Vibroseis Consortium has been provided by the following companies and governmental agencies: Amoco Production Co. (1 year), Arco Exploration Co. (2 years), Berea Oil and Gas Co. (1 year), Champlin Petroleum Co. (1 year), Chevron U. S. A. (2 years), Conoco Inc. (2 years), Gulf Oil Exploration and Production Co. (2 years), Mobil Exploration Co. (2 years), Nuclear Regulatory Commission (3 years), Phillips Petroleum Co. (1 year), Sohio Petroleum Co. (2 years), Sun Exploration Co. (1 year), Texaco, Inc. (2 years) and Virginia Division of Mineral Resources (1 year). Financial support in the form of assistantships and fellowships were provided by the Department of Geological Sciences at Virginia Tech, Chevron U. S. A., and Arco Exploration Co.

I would like to thank John K. Costain, my committee chairman, Gil A. Bollinger, and Lynn Glover for their involvement in the Virginia Tech Vibroseis Consortium. I would also like to thank the following people for their assistance is the preparation of this text: , and for assistance in processing the seismic data; for his work in the processing of Line VDMR1; , , , , and for their suggestions concerning the research involved in this text; and for the acquisition and processing of the earthquake data; and for the preparation of the text and drafting of the figures.

Most of all, I would like to thank my wife, , and my parents, , for their unending support.

TABLE OF CONTENTS

INTRODUCTION 1

VIBROSEIS DATA ACQUISITION AND PROCESSING 10

SEISMIC INTERPRETATION 22

DISCUSSION AND CONCLUSIONS 57

REFERENCES 59

Appendix A 63

Appendix B 66

Appendix C 70

Appendix D 74

Vita 75

LIST OF ILLUSTRATIONS

Figure 1. Location map of study area. 2

Figure 2. Geologic map of the study area with epicenters and seismic lines 3

Figure 3. Stratigraphy of Giles County County 7

Figure 4. Portion of VTVC Line 1 showing effects of crossdip . . 15

Figure 5. Portion of Line 1 after application of CDR 17

Figure 6. SH-wave reverberating energy recorded on common-shot gather 18

Figure 7. Stack (nonmigrated) of VTVC Line 2. 26

Figure 8. Interpretation of VTVC Line 2. 29

Figure 9. Stack (nonmigrated) of VTVC Line SH2. 31

Figure 10. Interpretation of VTVC Line SH2. 33

Figure 11. Stack (nonmigrated) of VTVC Line SH1. 36

Figure 12. Interpretation of VTVC Line SH1. 37

Figure 13. Stack (nonmigrated) of Line VDMR1. 39

Figure 14. Interpretation of Line VDMR1. 40

Figure 15. Stack (nonmigrated) of VTVC Line 1. 43

Figure 16. Interpretation of VTVC Line 1. 44

Figure 17. Previously published cross sections through the Bane Dome 45

Figure 18. Cross section A-A' through the area of study 46

Figure 19. Cross section B-B' through the area of study 47

Figure 20. Cross section C-C' through the area of study 48

Figure 21. Block diagrams based on previous cross sections . . . 52

Figure 22. Observed and calculated gravity profiles over the Bane Dome 53

Figure 23. Definition of crossdip and its effect on stacked data. 64

Figure 24. Local inhomogeneities within layers leading to time-variant shifts. 71

INTRODUCTION

The Virginia Tech Vibroseis Consortium (VTVC), an industry-university-governmental research group, was formed in 1982 to develop new methods of reflection seismic data acquisition, processing, and interpretation in the Appalachian region. Vibroseis data are obtained and analyzed using the Vibroseis and VAX 11/780 facilities at Virginia Tech.

From 1982-1984, Consortium-sponsored research was centered around the Bane Dome structure located in Giles County, Virginia in the southern Appalachians (Figure 1). The purpose of this study was twofold; first, to determine the structure and lithology of the supporting feature beneath the Bane Dome Complex and secondly, to determine the role of rejuvenated basement (Precambrian) faults as the cause of the current earthquake seismicity within the Giles County Seismic Zone (Bollinger and Wheeler, 1983).

A total of 40 km of predominately 24-fold Vibroseis data was acquired, including 24 km of P-wave data and 16 km of SH-wave data. Also integrated into this study are 13 km of 24-fold P-wave data, located approximately 20 km southeast of the Bane Dome, acquired by Virginia Tech for the Virginia Division of Mineral Resources (Stanley and Schultz, 1983).

This was the first study to integrate the surface geology with both P-wave and SH-wave reflection data to determine the geologic structure and history of this area. Emphasis was given to those autochthonous rocks

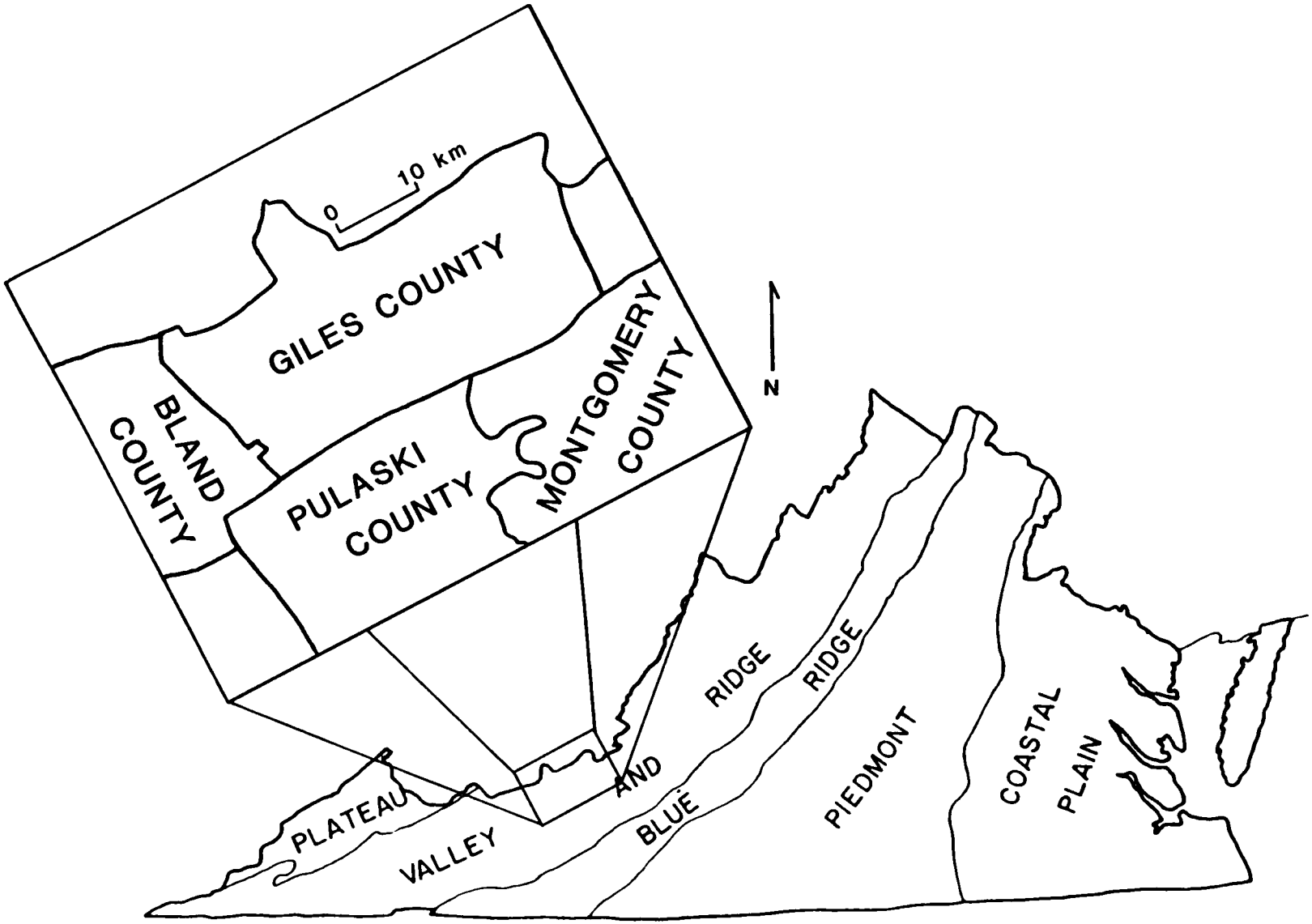

Figure 1. Location map of study area.

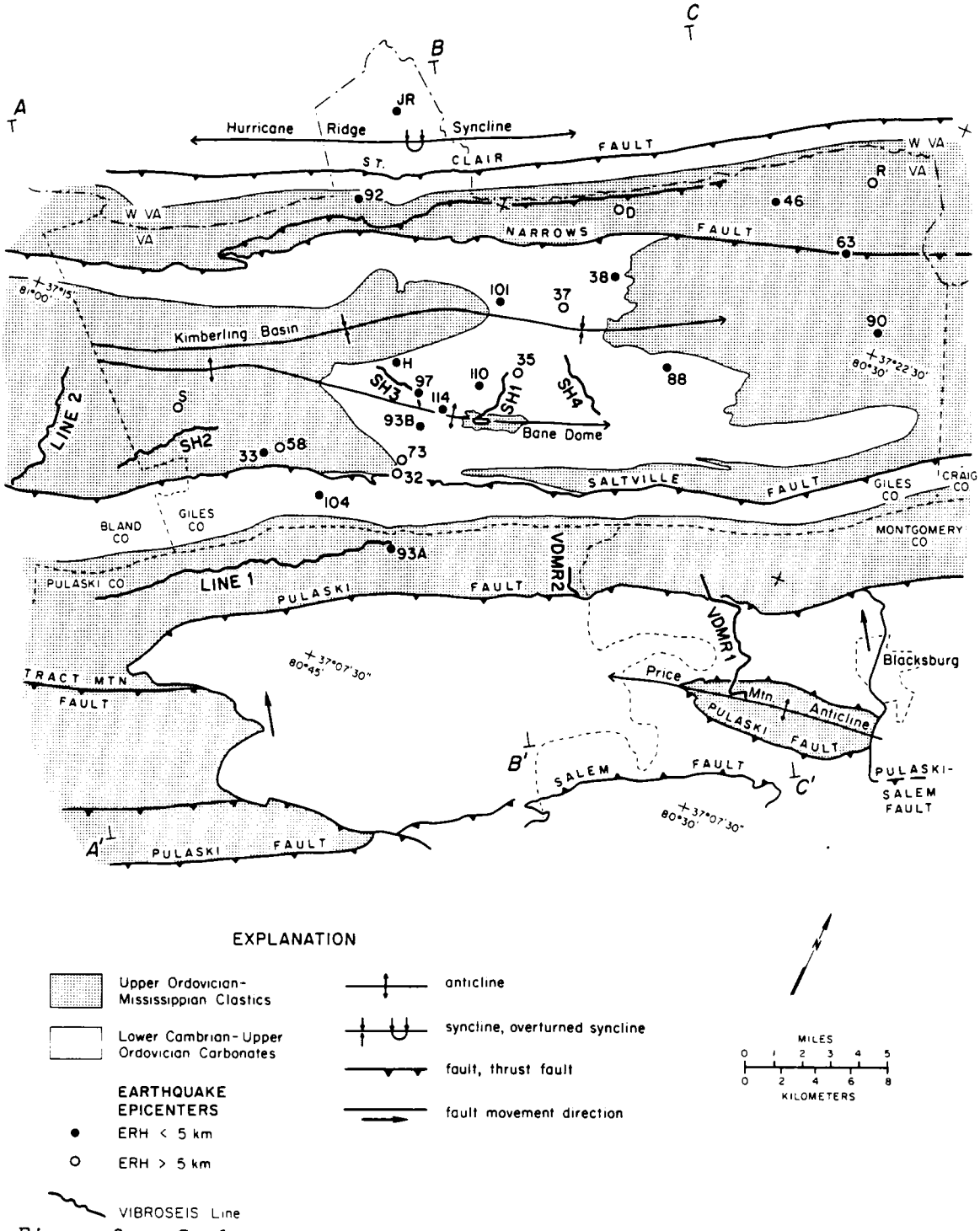

Figure 2. Geologic map of the study area with epicenters and seismic lines: Geology based on state geologic map of Virginia, Calver, 1963. Geology of Pulaski and Montgomery Counties from Schultz, 1983.

unaffected by the Alleghenian thrusting; specifically, the Precambrian basement rocks.

The area has historically been of interest to petroleum exploration companies since the 1940's. Interest waned because of early failures, such as the drilling of the Calco No. 1 Strader well on the crest of the Bane Dome, along with the higher cost of exploration because of the complex geology, rugged topography, and remote location from areas of current hydrocarbon production. Recent hydrocarbon discoveries in nearby West Virginia and eastern Tennessee have renewed interest in this portion of the Appalachian Basin.

Recent Seismicity

In addition to the interest in this area for hydrocarbon exploration, Giles County is of interest to earthquake seismologists because of its history of low level seismic activity (Bollinger and Wheeler, 1983). Activity is currently being recorded by a 7-station local network operated by the Virginia Tech Seismological Observatory. Twenty four events (Figure 2) have been located in the area since 1959, including nineteen recorded by the network between 1978 and 1984. The magnitudes of the events range from 0.0 to 4.0 with depths that range from 4 to 20 km. The location and frequency of the events led to the designation of this area as the Giles County Seismic Zone (Bollinger and Wheeler, 1983). Recent results of detailed location and focal mechanism studies suggest a set of faults in crystalline basement that trends N 20-27°E with near vertical dip and predominantly strike-slip movement (Munsey, 1984; Munsey and

Bollinger, 1984). The location and identification of these faults is important for the determination of the earthquake risk analysis in the southeastern United States (Bollinger, personal comm., 1985).

A regional crustal velocity model, based on seismic refraction studies, has been determined at the Virginia Tech Seismological Observatory (Bollinger et al., 1980). That Giles County crustal velocity model is composed of four layers. The shallowest layer, 5.7 km thick, has an average P-wave velocity of 5.63 km/s, a S-wave velocity of 3.44 km/s, and therefore an average V_p/V_s ratio of 1.64. This layer, because of its physical characteristics, is interpreted as representing the Paleozoic sedimentary rocks which overlay the Precambrian basement sequence. The next layer in the model has a thickness of 9 km, with an average P-wave velocity of 6.05 km/s, S-wave velocity of 3.52 km/s, and V_p/V_s ratio of 1.72 (Bollinger et al., 1980). As will be discussed later in the text, the velocities and thickness of the upper layer compares favorably with the results from the Vibroseis study. Because of the restricted offset distances and the lack of strong reflections in the granitic basement rocks, accurate values for the velocities of the deeper layers in the velocity models were unconstrained by this study.

General Geology

The study area is located within the Valley and Ridge Province of the southern Appalachians. The rocks exposed in the area are sedimentary and Middle Cambrian to Mississippian in age (Figure 3). The dominant

structures are thrust sheets with bordering faults that trend N60-65°E (Figure 2 Calver, 1963).

The thrust sheets are characteristically broad and synclinal, locally interrupted by domal structures. One such structure within the Narrows thrust sheet is the Bane Dome in Giles County, Virginia. The Bane Dome is a broad doubly-plunging anticline with a fold axis parallel to the dominant structural trend of the Appalachians in this region. The Bane Dome is bounded along strike on the southwest by the Kimberling Basin and on the northeast by Johns Creek Syncline. On the north, the Bane Dome is bounded by the Pearisburg Syncline, and on the south by the Saltville thrust (Calver, 1963). The dome is cored by the Middle Cambrian Rome Formation (Cooper, 1964) (Figure 2). At the crest of the Bane Dome is a window in which the younger Cambro-Ordovician Knox Group is poorly exposed (Perry et al., 1979). In areas where the Rome Formation is unfaulted, it is typically a 700 m thick mudstone with minor interbedded dolomites. In this area the Rome is always fault-bounded at the base by a thrust fault. The majority of the thrust faults in this region probably originate in the Rome (Perry et al., 1979).

Overlying the Rome are massive, bedded dolomites, over a thousand meters in thickness, with a few interbedded shales. These dolomites, the Upper Cambrian Honaker and the Upper Cambrian-Lower Ordovician Knox Group are the predominant lithologic units in the study area. The majority of the study area is directly underlain by dolomitic rocks because of the great thickness of these units and the broad structure of the Bane Dome. Near-surface dissolution of these dolomites is believed to be one of the causes of the poor quality of the seismic data in this area.

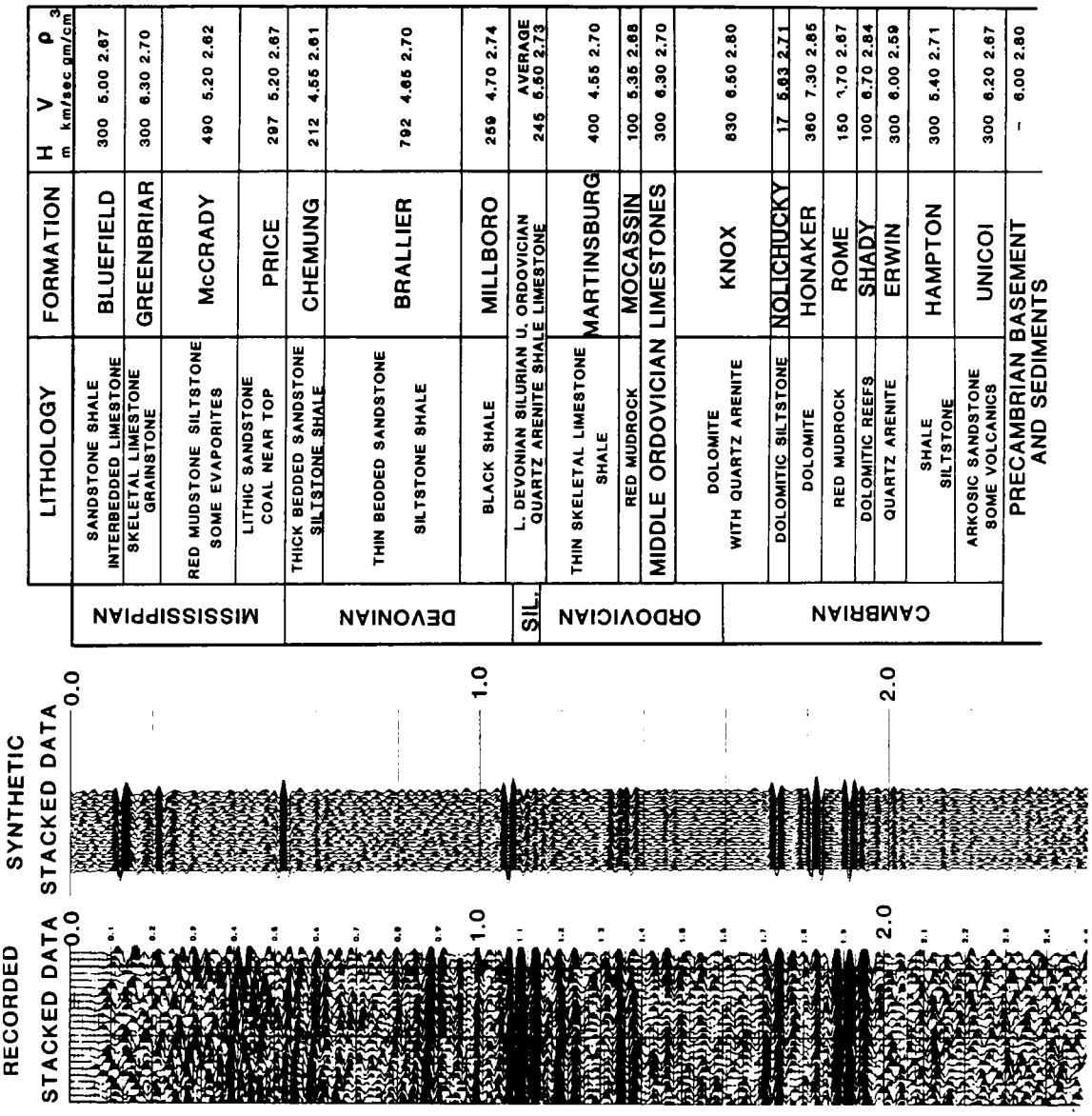

Figure 3. Stratigraphy of Giles County County: Recorded stacked reflection data compared to synthetic stacked section. Thickness and description of units from unpublished report of Virginia Tech's Carbonate Research Arctic/Appalachian Projects (CRAP) Laboratory, as well as Stanley and Schultz, 1983. Velocity and density values from Edsall, 1974 and Kolich, 1974.

Previous Work

In 1948, the California Company (Calco) drilled the F.P. Strader 1 on the crest of the Bane Dome with the objective of testing the structure for hydrocarbon potential. The drill site was located on the Rome Formation and the drill hole penetrated to a depth of 440 m. The base of the Rome was reached at a depth of 8.5 m at a pronounced contact between the Rome Shale and an underlying dolomite. The thickness of the Rome at the drillsite of 8.5 m confirmed that the Rome is approximately 100 m thick at Bane. Drilling was continued until it was terminated in a massive dolomite. Interpretation of the data (Cooper, 1964) suggested that the unit underlying the Rome Shale was the Shady Dolomite, the normal stratigraphic sequence, thereby implying a thick-skinned origin for the Bane Dome and related structures, although the thinness of the Rome Shale over the Bane Dome is not fully explained by thick-skinned tectonics.

Recent work based on conodont interpretations by Perry et al., (1979) suggested that the data were misinterpreted and that the unit underlying the Rome Shale was actually the younger Cambro-Ordovician Knox Group. This reinterpretation of the Bane Dome is consistent with the thin-skinned tectonic style of the Folded Appalachians.

Problems in Seismic Data Acquisition

With the recent renewed interest in this area, many kilometers of conventional (P-wave) seismic data were acquired by geophysical contractors in the area of the Bane Dome, but the data quality has been poor

because of 1) high-velocity limestones and dolomites that immediately underlie the area, and 2) karst topography.

Similar geologic settings, i.e., high velocity surface carbonates, have been observed to contain local areas of low quality P-wave data (Fix et. al., 1983). In some areas, e.g., the Val Verde and Delaware Basins of West Texas, high quality SH-wave data can often be obtained. During the acquisition of P-wave data in those areas, large amplitude surface waves and refracted P-waves are generated that obscure co-arriving reflected energy. It has also been observed that high quality shear-wave data can be obtained in such areas because virtually no Rayleigh waves are generated that can be detected on transverse horizontally polarized geophones; therefore, SH reflections are not obscured (Fix et al., 1983; Waters, K. H., personal comm., 1983). Love waves recorded on SH-wave data have not, thus far, been observed to be a problem in these areas.

The presence of near surface carbonate rocks, coupled with a high amount of precipitation, causes the Giles County, Va. region to be one of karst topography. This is yet another reason that P-wave data are poor in certain areas of the Appalachians. Near surface solution cavities and cavernous porosity have resulted in the observation of degraded P-wave data. Because this is the first SH-wave Vibroseis study in the Appalachians, it was not known if SH-wave data quality would also be poor.

VIBROSEIS DATA ACQUISITION AND PROCESSING

A location map of the seismic lines acquired by VTVC during 1982-83 and 1983-84 is shown in Figure 2. The field acquisition parameters and the geologic features of each line are described in Table I.

Data Acquisition in Problem Areas

The southern Appalachians is an area with a history of reflection seismic data acquisition problems. Steeply-dipping beds, mountainous relief, areas of high velocity surface rocks, and karst topography are examples of geologic problems. Narrow, crooked roads and areas of limited access cause geometric problems with the subsequent data processing. One objective of VTVC is to minimize these problems by developing new techniques of data acquisition and processing to insure the highest possible quality data.

P-wave Data Acquisition

VTVC Lines 1 and 2 (Figure 2) were the first seismic lines acquired by the Consortium. In order to optimize data quality, these lines were sited on areas underlain by clastic rocks. Multifold data were acquired using Virginia Tech's Failing Y-1100 P-wave vibrator as a single point source and a MDS-10 48-channel digital system with field summing capability and Min-Max vertically polarized 20-element geophone arrays.

TABLE I

Lines Acquired by the Virginia Tech VIBROSEIS Consortium (VTVC) 1982-1984

Line Name	Line Length	Line Type	Surface Geology	No., Type Vibrators	Sweep Range	Sweep Length	Sweeps per S.P.	Station Spacing	Near Offset
Line 1	18 km.	P-wave	Clastics	1 P	14-56 Hz.	24 secs	16	70 m	350 m
Line 2	6 km.	P-wave	Clastics	1 P	14-56 Hz.	24 secs	16	70 m	350 m
Line SH1	3 km.	SH-wave	Carbonates	2 SH	6-36 Hz.	24 secs	8	35 m	210 m
Line SH2	5 km.	SH-wave	Clastics	2 SH	10-40 Hz.	26 secs	8	70 m	420 m
Line SH3	3 km.	SH-wave	Carbonates	2 SH	10-40 Hz.	26 secs	8	35 m	210 m
Line SH4	5 km.	SH-wave	Carbonates	2 SH	10-40 Hz.	26 secs	8	35 m	210 m

SH-wave Data Acquisition

In December, 1983, as part of the second year of the Consortium, four SH-wave Vibroseis lines totaling approximately 16 km of 24-fold CDP data were acquired on and around the Bane Dome. The lines are designated SH1 to SH4 in Figure 2.

Data were acquired using two Conoco shear-wave vibrators and recorded using horizontal geophones and the above mentioned recording system. To allow for easier event correlation between P-wave and SH-wave data, the sweep used for the SH-wave study contained half the frequencies of the P-wave sweep (Table I). Each sweep was individually recorded (no summing in the field).

A severe statics problem was noted in early shear wave surveys (Erickson et al., 1968). In an attempt to minimize such statics problems in this survey, individual sweeps were closely spaced. Eight sweeps per source point per vibrator pair were used on all SH-wave lines. An initial ("blurp") sweep was made to insure proper coupling with the ground, after which two sweeps were made in each pad position. To insure that adjacent sweeps could be summed together without degrading data quality, new pad positions were located immediately adjacent to the previous position.

Shear vibrators have large steel cones fixed to the base plate that are forced into the road bed. The SH-wave vibrator vibrates in a horizontal direction, and the cones are necessary to insure proper ground coupling. In the past, these vibrators were used only in areas of low relief where data can be acquired in off-road areas, away from dwellings and roads. The mountainous relief in Giles County prohibited this method

of data acquisition, and the vibrators were used only on secondary unpaved roads that could be restored to their original condition upon completion of the survey. This complication caused restrictions on the location as well as the length of shear-wave lines. The results, in general, justified the additional time and effort involved in the acquisition of shear wave data.

Seismic Processing

As previously mentioned, this portion of the United States offers many challenges to the acquisition of reflection seismic data. The following portion of the text is a brief description of the type of problems which became evident while processing this seismic data. Detailed discussions on the processing of the data can be found in the designated appendices.

Removal of Crossdip effects

VTVC Line 1 was a strike line located over the Devonian clastic sequence (Millboro and Brallier Formations) in Pulaski County, Virginia. Structurally, it was on the hanging-wall of the Saltville thrust sheet approximately 6.5 km southeast of where the fault crops out. From surface mapping, the rocks within the Saltville sheet along the seismic line dip approximately 35° to the southeast. After conventional processing of Line 1, it was noted that the reflections in the final stack suggested shallow geologic structure inconsistent with exposed surface geology. It was

suspected that the relative orientation of the roads with respect to near surface structure might have affected reflection arrival times.

In this area, seismic lines must be acquired along available roads which tend to be crooked. Along Line 1, the crooked road was approximately along strike and the rocks were steeply dipping. If a common-depth-point (CDP) is located off a straight line defined by the strike of the rocks, successive CDPs will show the same reflection arriving at slightly different times. These crossdip variations in arrival times result in time shifts which create apparent structure on the seismic section. The values of these time shifts are dependent on the component of dip normal to the road (Larner et al., 1979).

A portion of VTVC Line 1 is shown in Figure 4 with a steeply dipping reflector marked "D". The dipping character of the reflection denote apparent structure caused by crossdip. These apparent updip or downdip reflections resulted in the final stack as a function of the trend of the survey line. The more the survey line deviated perpendicularly from the line of strike, the greater the effects of crossdip. As the survey line trended toward the north, up dip, the reflections will have earlier arrival times, while deviations of the survey to the south would cause reflections to have greater arrival times. Two-dimensional displays of these reflections causes an apparent dipping of the reflections.

It is noted on Figure 4 that the crossdip effects diminish with depth. By projecting the surface geology into the subsurface and from seismic signature interpretation of Line 1, it is interpreted that the Saltville Fault cuts through Line 1 at approximately 1.2 s two-way travel-time. From the interpretation of a seismic cross-tie line (VDMR1),

Figure 4. Portion of VTVC Line 1 showing effects of crossdip: Processed using normal processing sequence. Note dipping reflection marked "D" . Apparent structure believed caused by crossdip.

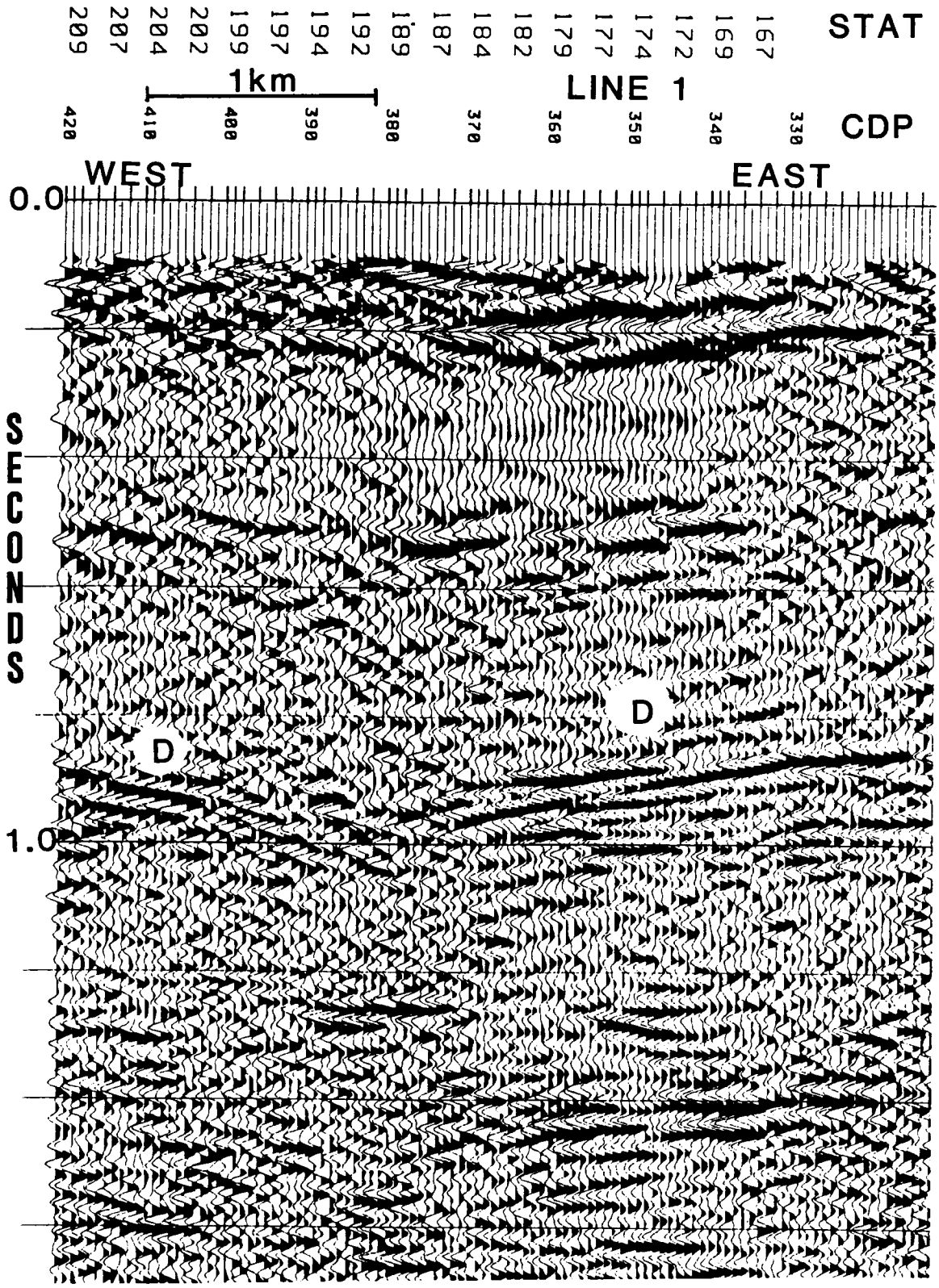
STAT
209 207 204 202 199 197 194 192 189 187 184 182 179 177 174 172 169 167
1km
LINE 1
CDP
420 410 400 390 380 370 360 350 340 330
WEST
EAST
0.0
SECONDS
1.0
D
D

it is known that below the Saltville thrust sheet the underlying rocks are nearly horizontal, and are therefore less affected by crossdip effects. Because of this complex geology, the method of crossdip removal used must be able to remove the effects of crossdip as a function of depth, so that reflections unaffected by crossdip effects will not be disturbed.

For Line 1, software called Crossdip Removal (CDR) was developed and used by VTVC to remove the effects of crossdip. For a detailed explanation of Crossdip Removal, see Appendix A.

The results of CDR are shown in Figure 5. Note the removal of the apparent structure caused by crossdip, while not affecting the deeper events (those deeper than 1.2 s). Previous methods of crossdip analysis (Larner et al., 1979) allowed only a static shift of each trace to compensate for crossdip effects. CDR allows time variant shifts which remove the crossdip effects caused by a single layer or group of dipping layers without disturbing those reflections in other portions of the trace unaffected by crossdip.

Care should be taken when interpreting this line. Reflection points from a line which has CDR applied will lie in the normal incidence strike plane, and not along the road as described by the line geometry.

Removal of Reverberations

A typical common-shot gather of a shear-wave Vibroseis line (VTVC Line SH1) acquired directly over the Bane Dome is shown in Figure 6. The

Figure 5. Portion of Line 1 after application of CDR: Note the increased coherency of reflections and the removal of the apparent structure.

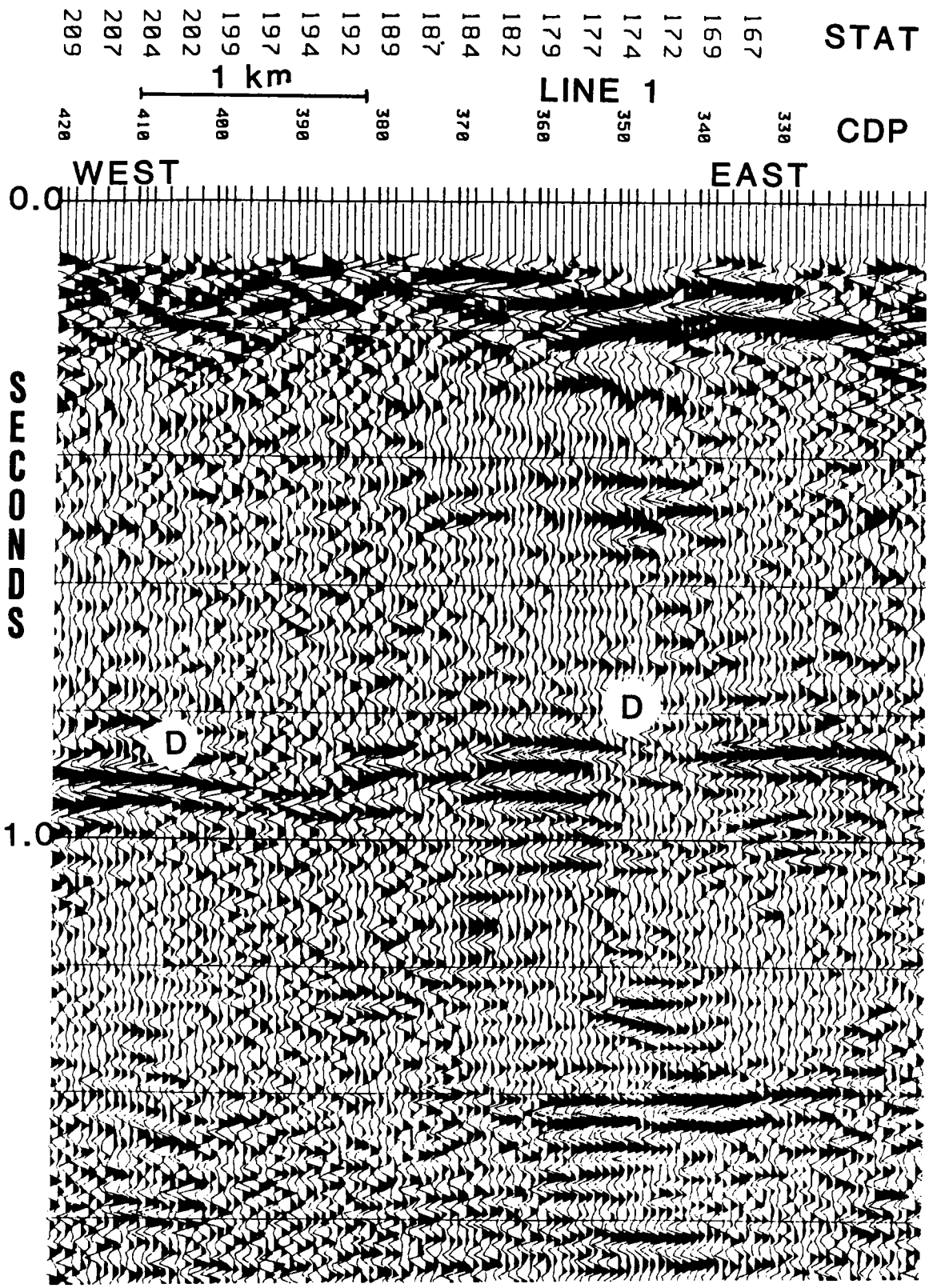
209 207 204 202 199 197 194 192 189 187 184 182 179 177 174 172 169 167
STAT
1 km
LINE 1
420 410 400 390 380 370 360 350 340 330
CDP
WEST
EAST
0.0
SECONDS
1.0
D
D

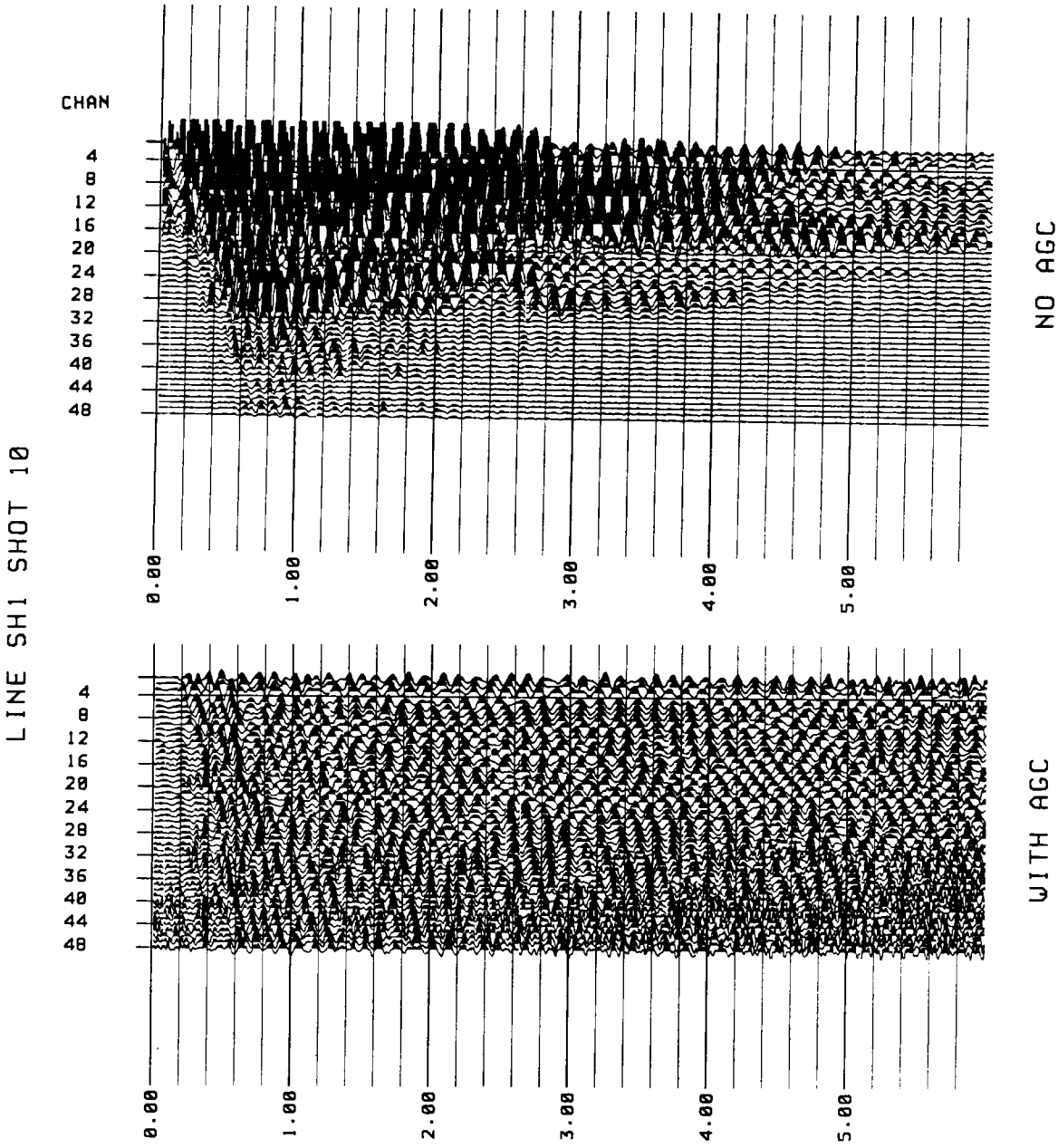

Figure 6. SH-wave reverberating energy recorded on common-shot gather: Shot gather along SH-wave Line SH1, recorded on the crest of the Bane Dome.

reverberating energy in the shot record completely masks the arrivals of the primary reflections.

The near surface geology underlying the Bane Dome is one in which two high velocity dolomites (Honaker and Knox) overlay and underlay a fault-bounded low-velocity shale (Rome). On the north flank of the Bane Dome, where Line SH1 is located, the Rome and the overlying Honaker both dip approximately 20°N.

The high velocity contrast between the Rome Shale and its surrounding dolomites act as an effective wave guide to trap energy within the Rome. Because the wave-guide is inclined, the reverberations generated within the Rome change in character along the line. For these reverberations, unlike the well known reverberations in marine data, the wave-guide was a lithic unit; therefore, the velocity of the reverberations was almost the same as the velocities of the primary reflections. Because of this, neither stacking nor velocity filtering yielded adequate suppression of the unwanted reverberations.

Multiple runs of gapped predictive deconvolution over selected time intervals with numerous changes in deconvolution parameters would be necessary to remove the spatially and temporally varying reverberations. Thus, it was decided to seek an alternative method to remove the reverberations.

Because of the varying characteristics of the reverberations, it is desirable to use a method of deconvolution which is similar to gapped deconvolution, but more flexible. An alternative to gapped deconvolution was first discussed by Ristow and Jurczyk (1979) who suggested using a minimum-phase filter on Vibroseis data to alter the phase spectrum so that

a minimum-phase assumption could be made for the source wavelet. Spike (unit distance) predictive deconvolution can then be applied to remove the reverberations. A discussion of minimum phase filter deconvolution is found in Appendix B.

Multiple problems were noted on all SH-wave lines; however, only SH1 exhibited reverberations. Minimum phase filtering/spike deconvolution was used on all SH-wave lines acquired on carbonate rocks, with excellent results.

Residual Statics Analysis

Erickson et al., (1968) first discussed the importance of residual statics analysis for SH-wave data due to the longer time spent in the weathered zone and their sensitivity to lateral variations in velocity and density within this layer.

After completion of a normal processing sequence of the SH-wave data, it was noted that small time-variant delays (less than 20 ms) had been applied to the data traces. These delays, believed to have been caused by localized inhomogeneities, cannot be removed by normal residual statics analysis, therefore, an alternative processing approach was used to remove these shifts.

Residual statics were independently calculated for individual time windows along the length of the seismic section. The statics were then applied to their respective data sets. After application of the statics, the individual data sets were summed together. After summing, additional velocity and standard residual statics analysis were applied. In all

cases, this procedure was found to be superior to standard processing techniques. A detailed explanation of this method of residual statics analysis can be found in Appendix C. This technique has been applied to all final SH-wave record sections for this study.

SEISMIC INTERPRETATION

Seismic Marker Horizons

The only drill holes in this area either predate modern geophysical techniques or are of insufficient depth to determine formation boundaries. Methods other than direct identification must therefore be used to interpret lithology and depth to reflectors.

Methods of interpretation used in this study included projecting surface dips into the subsurface, using seismic lithostratigraphic relationships from adjacent areas with borehole control, and seismic modeling of the assumed geologic model using thicknesses inferred from surface geology and laboratory derived velocity determinations.

One such synthetic generated using modeling software SOLID® (Trade mark of Geophysical Development Corporation) is shown in Figure 3. (This figure and all figures of seismic sections in this text are plotted with two-way travel-time on the vertical axis. For a conversion from travel-time to depth, an appropriate conversion factor is 1 second ≈ 3 km depth for P-wave and 1 second ≈ 1.8 km for SH-wave data.) SOLID is a software program which creates synthetic traces as a function of time and offset. Calculations are carried out in the f-k domain using a modified Thompson-Haskell matrix method. A P-wave line source is assumed.

Formation thicknesses, used as input for SOLID, were based on observed surface geology (Stanley and Schultz, 1983). The velocities were determined in the Regional Geophysics Laboratory at Virginia Tech from

representative rock samples (Edsall, 1974; Kolich, 1974). Ten percent random noise was added to the synthetic model.

The synthetic stacked section compares favorably with the recorded seismic section acquired in a nearby portion of West Virginia, provided courtesy of Petty-Ray Geophysical. The geologic section modeled is in an area that has not been cut by major thrust faults. Differences between the actual and modeled data are due probably to the fact that the synthetic was generated assuming constant velocity and density throughout the formation.

Although the distinctive seismic markers in Giles County tend to be few in number, they are easily recognized (Figure 3). There are three predominant seismic markers in this study area. They are the Cambrian Rome Formation, the Cambrian Nolichucky Formation and a sequence of Devonian, Silurian and Ordovician units (DSO sequence).

The entire Cambro-Ordovician sequence has a distinctive seismic character and can be easily recognized. The Knox Group, which are thick-bedded dolomites, are typically high P-wave velocity rocks with discontinuous reflections (Figure 3). Immediately below the Knox Group is the Cambrian Nolichucky Formation. The Nolichucky in this area is a dolomitic siltstone with a relatively low velocity when compared to the overlying Knox. The Nolichucky is only approximately 17 m thick where it is found at the surface in this area (Stanley and Schultz, 1983). Directly underlying the Nolichucky is the Cambrian Honaker Dolomite. This is another high velocity, predominantly dolomitic unit. The thinness of the Nolichucky (nearing the tuning thickness for a Vibroseis wavelet) and the strong negative and positive impedance contrasts at its upper and

lower formational contacts, respectively, make this one of the most distinctive reflections in the subsurface of the eastern United States (Figure 3).

In the normal stratigraphic sequence, the Honaker Dolomite is underlain by the Rome Formation, which is itself underlain by the Shady Dolomite. The Rome is an approximately 100-700 m thick unit composed predominantly of shale with some interbedded dolomites. As with the Nolichucky, the Rome is a low velocity unit which is overlain and underlain by relatively higher velocity units. The thickness of the Rome allows two distinct reflections to be generated. The upper contact has a strong negative impedance contrast, while the lower contact has a strong positive impedance contrast. The resulting negative and positive reflections can be seen on both the recorded stack and the synthetic stack (Figure 3).

The Upper Ordovician-Silurian-Lower Devonian sequence (DSO), which consists of thin to massive interbedded sandstones and quartzites (Silurian Tuscarora, Rose Hill and Keefer Formations), shales, cherts and limestones (Upper Ordovician Junita, Devonian Tonoloway, Needmore and Huntersville), also has a distinctive seismic character. The DSO sequence's seismic character, due to the relative thinness of the units (average thickness is 27 m) and the fairly strong impedance contrasts at the formational boundaries, tends to be a multiple set of reflections within a small time window (Figure 3).

Other reflections which are also evident on both the stacked section and the synthetic model and which aid in interpreting seismic sections, but are not as distinctive as the above mentioned reflections, are the

reflections from the Ordovician sequence (Martinsburg and Mocassin Formations and the undivided Middle Ordovician limestones) (Figure 3).

Using the synthetic section, which integrates the known lithostratigraphic section with the velocities and densities determined in the laboratory, it it was possible to interpret the seismic sections in the absence of borehole data.

Seismic Interpretation

The locations of the seismic lines acquired by the Consortium were governed by a number of factors. To optimize data quality, the P-wave lines were located in areas directly underlain by clastic rocks. Shear-wave lines were located on both clastics and carbonates and were dependent upon the availability of secondary unpaved roads. All seismic lines were located in close proximity to the Bane Dome; attempts were made to locate the lines along the trend of the Giles County seismic zone (Figure 2).

VTVC Line 2 was a P-wave line located along strike from the Bane Dome and near the recorded earthquake activity. Its location on the DSO clastics resulted in excellent data quality (Figure 7). This figure is a final nonmigrated stack of Line 2.

Distinctive reflections at 1.5-1.8 s two-way travel-time match the character previously described for the Cambrian sequence, specifically the Nolichucky and Rome formational contacts. Because of the arrival times and coherency of these reflections, they are interpreted to be from an

Figure 7. Stack (nonmigrated) of VTVC Line 2.: Stack of P-wave line located on the clastic rocks of the DSO sequence. Note the strong coherent reflections at 1.5-1.8 s, interpreted as autochthonous Cambro-Ordovician units beneath the major thrust faults seen at the surface.

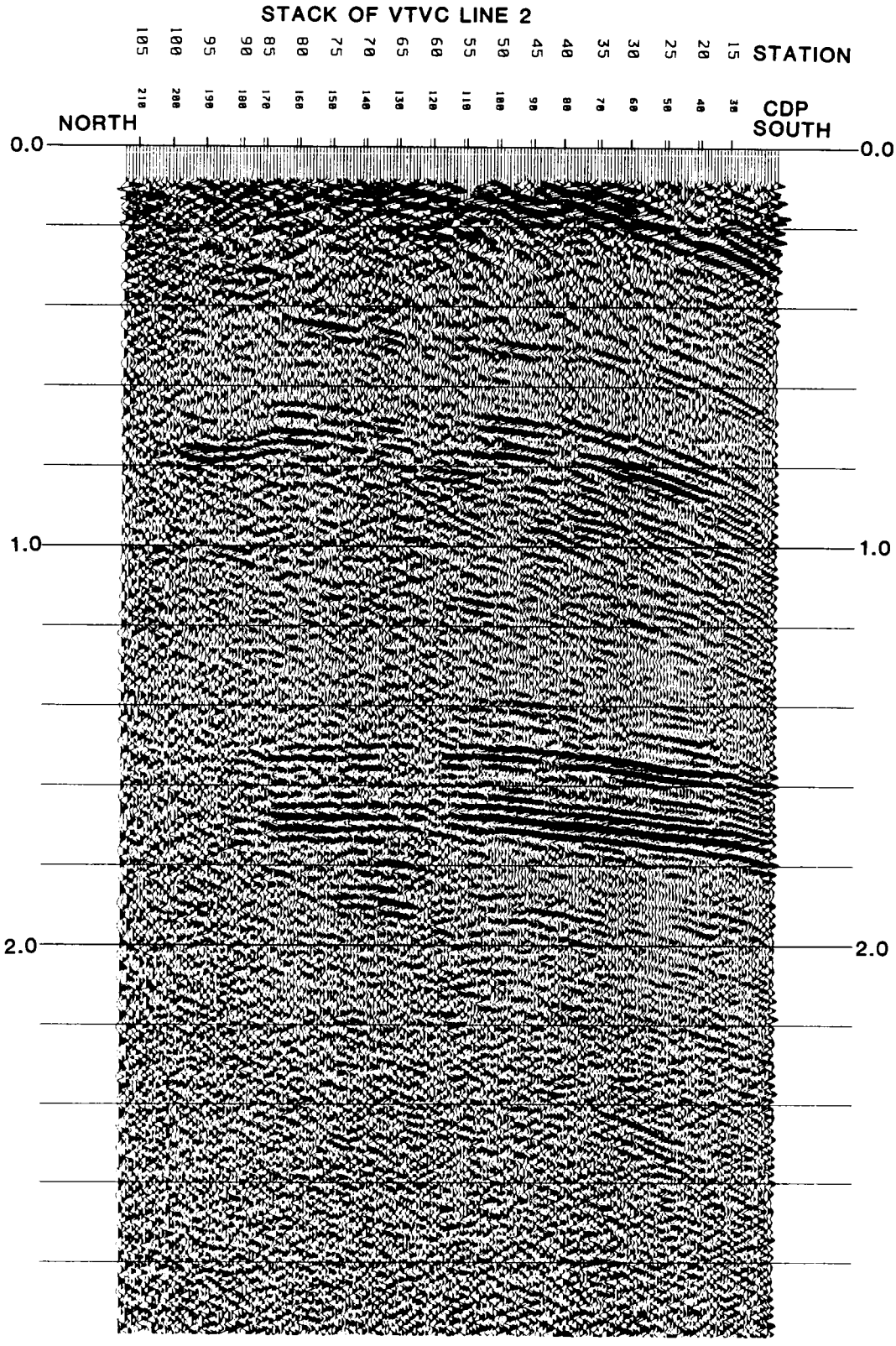
STACK OF VTVC LINE 2
STATION
CDP
NORTH
SOUTH
0.0
1.0
2.0

autochthonous sequence not involved in the major thrusting seen at the surface.

The character of the reflections become different farther up in the section. As noted in Figure 7, the reflections from 0.7-0.9 s are continuous and numerous. These reflections are similar to those reflections in the Upper Ordovician and DSO sequences as seen in the type seismic section (Figure 3). Minor offset of these units is interpreted as small thrust faults which noticeably displace the DSO reflections.

A distinct change in character is noted cutting obliquely across the seismic section, from 0.7 s at the north end of the line, to 1.3 s at the southern end of the line. This boundary is marked by truncation of reflections and a discordance of dip of adjacent reflections. This boundary is interpreted to mark the trace of a ramp structure on the footwall block of a thrust fault. Correlation of the DSO sequence on either side of the fault suggests that the throw is small, probably on the order of hundreds of meters. The DSO sequence on the hanging wall block of this ramp fault has been thickened by the minor thrust faults.

The DSO sequence crops out along Line 2. Those allochthonous rocks have been overthrust along one of the major faults in this area (Figure 2). Projecting surface dips into the subsurface, the reflection dipping to the south from 0.1 to 0.3 s is interpreted to be a reflection from within the Ordovician Martinsburg Formation. Below this reflection, the character of the reflections are similar to those of the Cambro-Ordovician sequence suggesting that another sequence of rocks, from Cambrian to DSO, is overthrust onto a sequence of the same rocks.

The interpretation of Line 2 is shown in Figure 8. A major thrust is interpreted to pass through this section, directly above the DSO sequence at 0.7-0.9 s. The DSO and the Middle Ordovician, Om, sequences at 0.7-0.9 s are completely bounded by thrust faults; a major roof thrust (interpreted as the St. Clair Fault), and a floor thrust fault with less offset. Such a feature is defined as a horse (Butler, 1982). This feature will be designated as horse "a" for the remainder of this paper.

Also useful in the interpretation of this seismic line are the P-wave interval velocity, V_p, the SH-wave interval velocity, V_s, and the ratio of the two velocities, V_p/V_s. The velocities and their ratios (Table II) were used in this study for a preliminary determination of lithology.

The calculated velocities and ratios for Line 2 are shown in Figure 8. Shear-wave velocities along Line 2 were derived from stacking velocities determined along VTVC Line SH2, which is located approximately 5 km along strike from Line 2 (Figure 2). The shear-wave reflections found on Line SH2 can be correlated with those on Line 2 (Figure 7 and Figure 9). Because Line SH2 is a strike line and correlations can be made between the reflections on each line, the velocities for the two lines were compared. In Table II are V_p/V_s ratios for common sedimentary rocks (McCormack et al., 1984). Note that the calculated V_p/V_s ratios correspond to the lithologies interpreted for Line 2.

TABLE II

LITHOLOGY	V_p/V_s RATIOS
Sandstone	1.5-1.9
Limestone	1.71-2.75

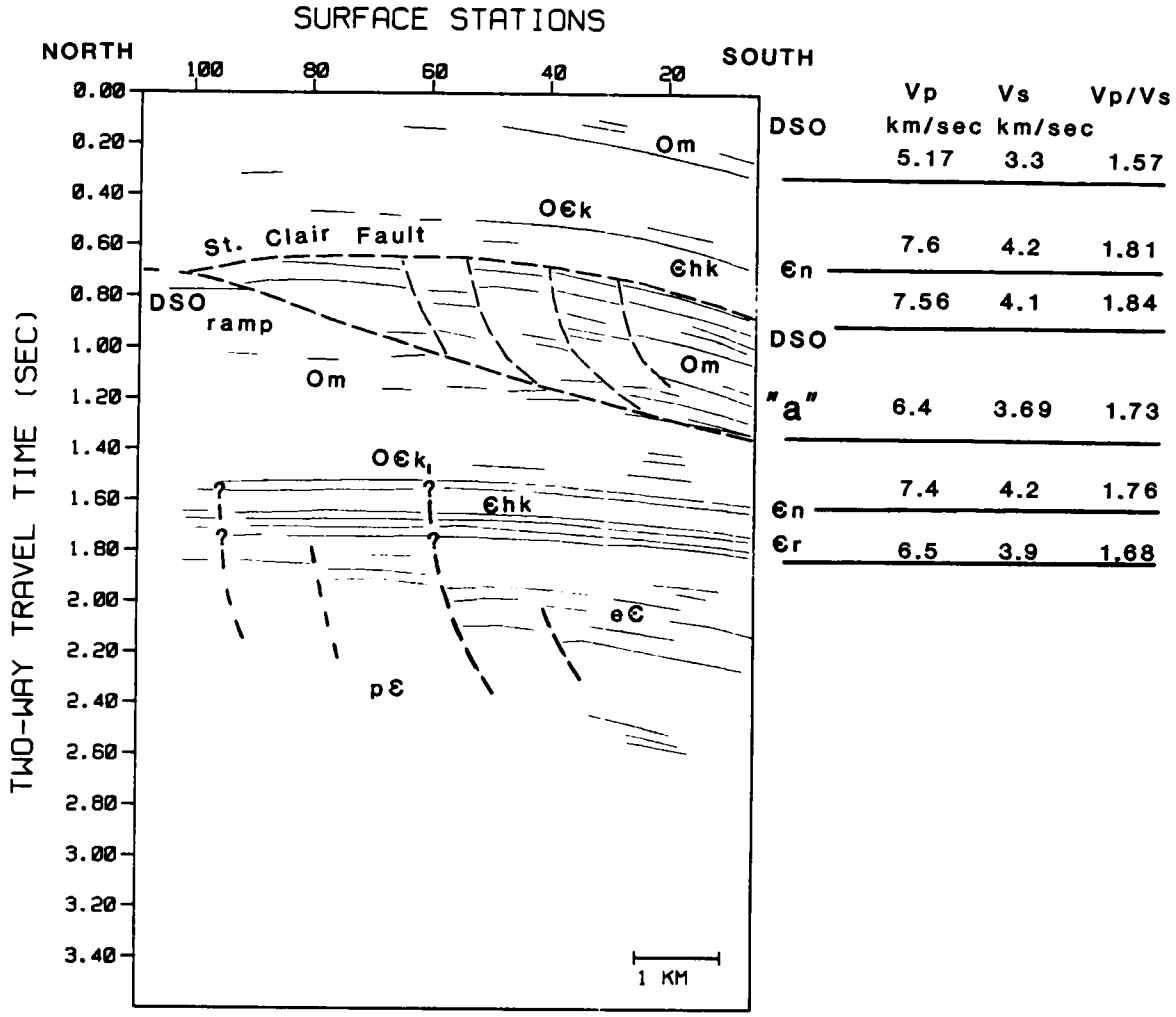

Figure 8. Interpretation of VTVC Line 2.: Included are P-wave and SH-wave interval velocities and Vp/Vs ratios. Interpreted geometry of horse block "a" with minor interal thrust faults. Also note interpreted normal faults in the Eocambrian sediments below 2.0 s which might extend into the Cambro-Ordovician sequence.

Shale 2.43-2.7

Dolomite average= 1.8

Difficulties arise when using V_p/V_s ratios in areas with low signal-to-noise ratios and a large statics problem. Statics problems decrease the accuracy of stacking velocity analysis and therefore increase the possibility of large errors in the V_p/V_s estimates. As it is known that velocity analysis becomes less accurate at increased travel-times, due to limited offset distances and decreased signal-to-noise ratios, V_p/V_s ratios begin to lose their significance at greater travel-times. For this study, it appears that the V_p/V_s ratios are consistent with the geologic interpretation to approximately 1.5 s P-wave two-way travel-time. Below this time, which is approximately 4.6 km in depth (assuming an average P-wave velocity of 6.2 km/s), the V_p/V_s ratio appears to have a constant value of 1.75.

P-wave velocities from the Vibroseis study ranged from 5.0 to 6.5 km/s for the predominantly clastic units, and from 6.5 to 7.6 km/s for the dolomitic units, (for an approximate P-wave velocity of 6.2 s), while SH-wave velocities ranged from 3.3 to 4.2 km/s. The thickness of the Paleozoic section in this area appears to be variable, but is approximately 5 to 7 km thick. From the Vibroseis study, an upper layer of the crust in Giles County is modeled as having the following parameters: thickness = 5 to 7 km, average P-wave velocity = 6.2 km/s, average SH-wave velocity = 3.75 km/s, and V_p/V_s ratio = 1.65. This local model compares favorably with the more regional Giles County velocity model of Bollinger et al., (1980) where the upper layer is modeled as: thickness = 5.7 km,

Figure 9. Stack (nonmigrated) of VTVC Line SH2.: SH-wave stacked section acquired over clastic rocks of the DSO sequence. Events correlate well with reflections found on P-wave Line 2 at twice the travel time, due to the slower velocity of SH-waves.

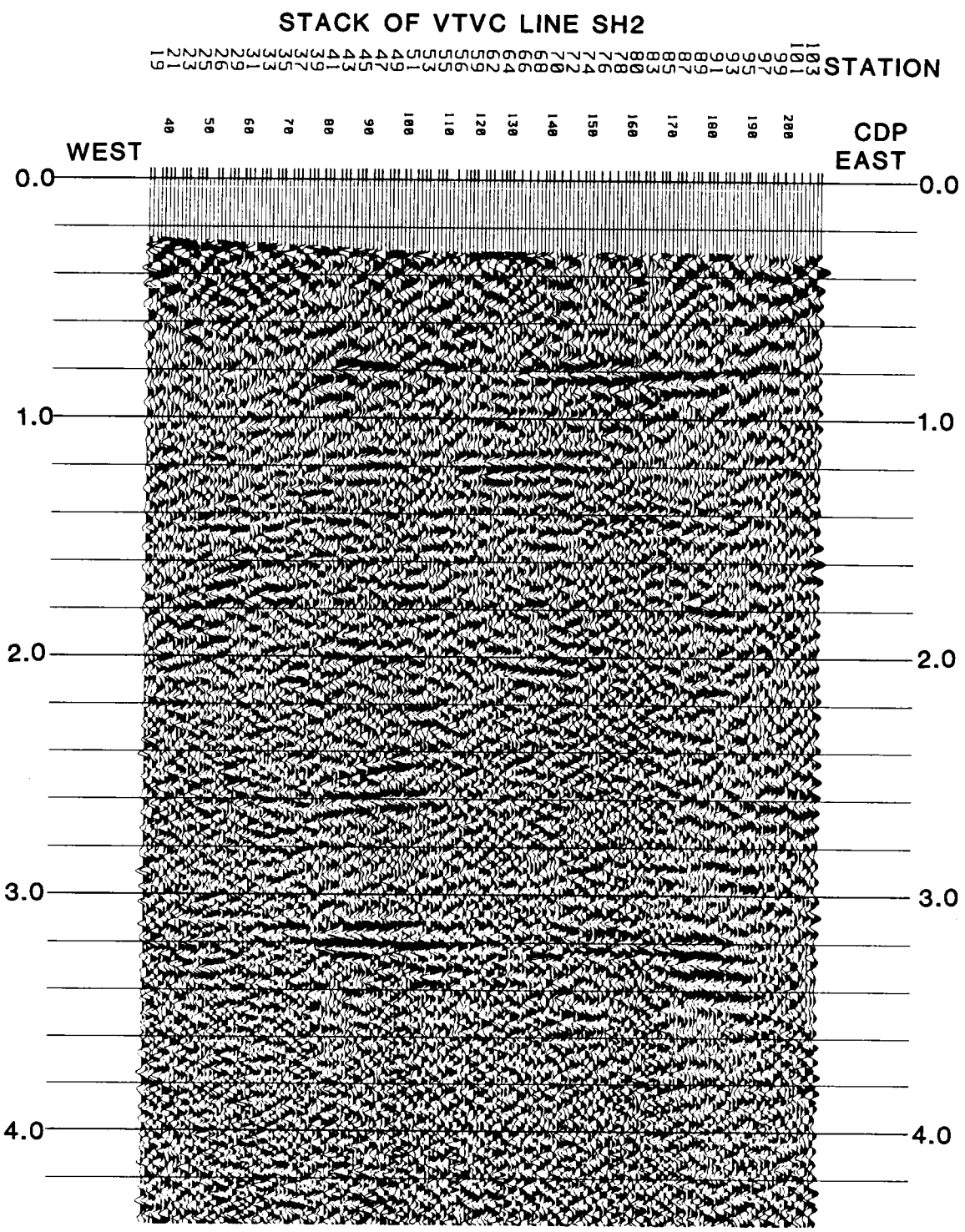
STACK OF VTVC LINE SH2
STATION
WEST
CDP
EAST
0.0
1.0
2.0
3.0
4.0
40
50
60
70
80
90
100
110
120
130
140
150
160
170
180
190
200

average P-wave velocity = 5.63 km/s, average S-wave velocity = 3.44 km/s, and an average V_p/V_s ratio = 1.64. In general, the velocity model derived from the Vibroseis study compares favorably to the model determined from earthquake studies, especially with respect to the V_p/V_s ratios. Because the Vibroseis study was centered in localized areas underlain by the higher velocity carbonate rocks, the average velocities determined from the reflection study are higher than those in the Giles County velocity model. Additionally, the Giles County velocity model was determined from seismic refraction surveys. Such surveys sample in a predominantly horizontal manner while reflection surveys sample in a vertical fashion.

As was previously mentioned, SH-wave Line SH2 was located approximately 5 km along strike from Line 2 (Figure 2). The line is located in the southern portion of the Kimberling Basin in clastic rocks of the DSO sequence. A stacked section of Line SH2 is shown in Figure 9. Note the good correlation of events between this line and P-wave Line 2. The reflection from the Nolichucky appears to be well developed on this line. Note that all reflections are fairly flat lying, suggesting that the structure present on Line 2 continues on strike toward the northeast and the Bane Dome at approximately the same depth. Because Line SH2 is a strike line (for the allochthonous units at the surface), the thrust faults identified in Line 2 will most likely not display any obvious displacement. An interpretation of the reflections of Line SH2 is shown in Figure 10.

In general, the data quality of Line SH2 was considerably better than other SH-wave lines. This is attributed to the fact that Line SH2 was acquired in an area underlain by clastic rocks. In some cases, sections

Figure 10. Interpretation of VTVC Line SH2.: SH-wave line located along structural strike from P-wave Line 2. Note the continuity of structures along strike as well as the interpreted normal faults cutting through the Cambro-Ordovician sequence.

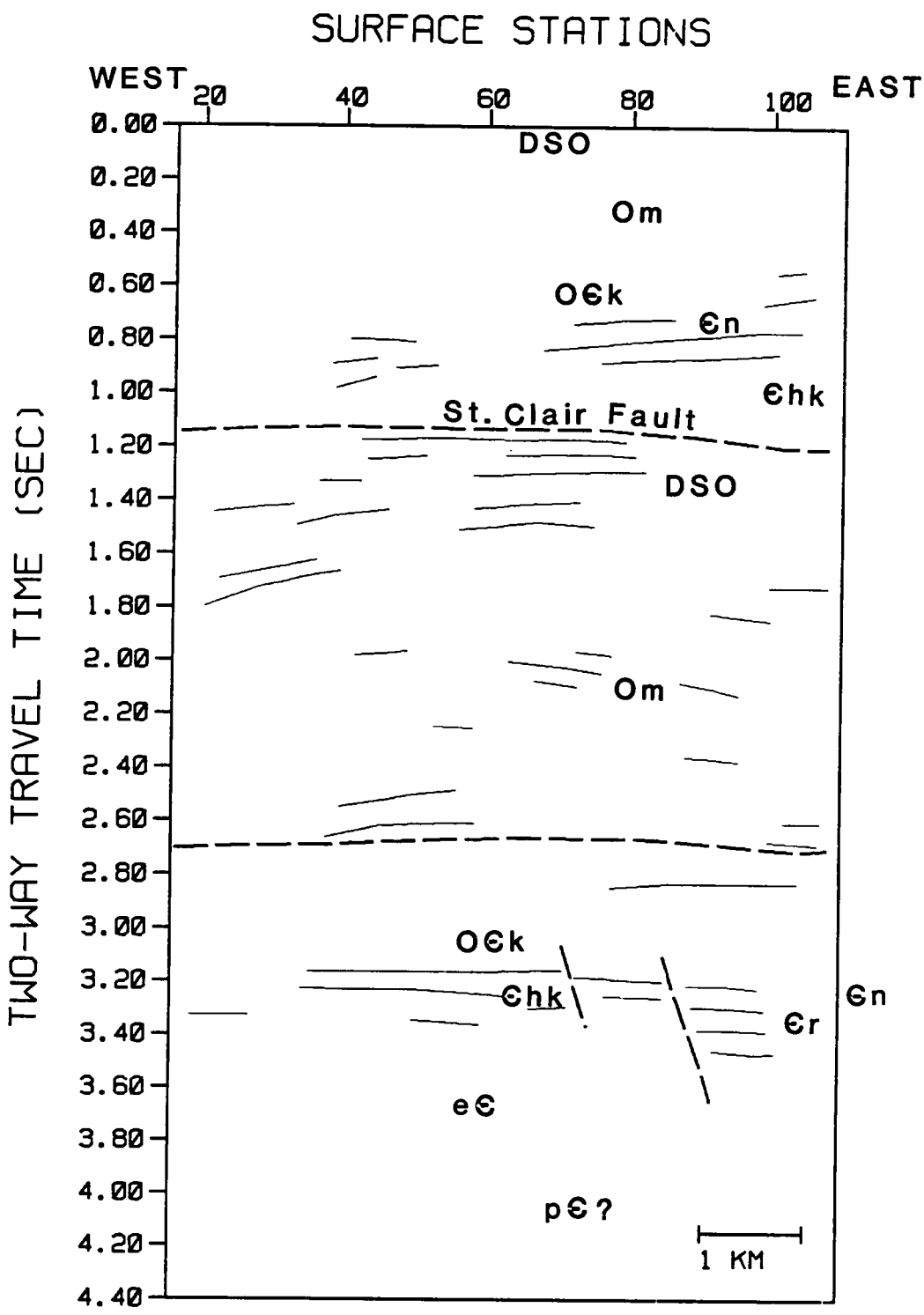

INTERPRETATION OF VTVC LINE SH2

of Line SH2 were of comparable quality to Line 2. The variation in the data quality of Line SH2 is believed to have been caused by the crooked nature of the road.

Unlike P-waves, SH-waves are polarized in the horizontal plane and they exhibit varying particle motions depending on the angular relationship between source and receiver. For the case where the vibrator vibration direction and the geophone polarization are parallel, the recorded SH-wave reflections will have the highest amplitudes. Any deviation will cause lower amplitude reflections to be recorded. At the point where vibrator direction and geophone polarization are perpendicular, no reflected SH-waves will be recorded. The areas of poorer data quality along Line SH2 relate to portions of the road which are the most crooked. Along those parts of the road, the vibration direction and polarization direction of the geophones were not parallel and therefore the signal-to-noise ratio expectably decreased.

SH-wave Line SH1 was located on the crest of the Bane Dome (Figure 2) upon the massive Cambro-Ordovician dolomites. Because Line SH1 was sited on carbonate rocks, the data quality is poorer in comparison with the other lines; however, this SH-wave line is still far superior to known P-wave data in this area acquired on carbonates. The karst topography in this area is highly variable and the portions of Line SH1 where the data quality is poorest are probably areas of heaviest karst development.

On Line SH1 (Figure 11), reflections which are similar to those found on Line 2 and Line SH2 are seen at 2.8-3.2 s. These reflections appear to correlate well with the Nolichucky and Rome reflections. Again, it

appears that the complete Cambro-Ordovician sequence is present on this line. Other reflections of interest on this line are the dipping reflections from 1.0-1.4 s. These semi-continuous reflections are dipping to the south, and have the same general character as the DSO sequence found on Line 2. Also evident is a discontinuity of the reflections similar to the ramp structure found on Line 2. The interpretation of Line SH1 is that there is a horse feature present on Line SH1 which is identical to the horse found on both lines SH2 and Line 2. In the interpretation of Line SH1 (Figure 12), this feature is interpreted as horse "a".

On the surface, at the southern portion of Line SH1, the window which exposes the Knox Group through the Narrows thrust sheet is found. Therefore, there is an additional thrust which passes through the seismic section, near the surface, bringing the Knox Group and other rocks over horse block "a" . This fault, though not visible on this seismic section, has been sketched in on the interpretation. This additional block, which has the St. Clair fault as a floor thrust and the fault exposed in the window as a roof thrust, is designated block "b" . Horse block "b" has a more limited extent along strike than horse "a" , interpreted because horse block "b" is not apparent in seismic sections Line 2 and Line SH2. Block "b" is a second horse block which has been placed upon horse "a" during thrusting, creating a duplex structure.

The results of the other SH-wave lines were not of the same quality as SH-wave Lines SH1 and SH2. On SH-wave Line SH4, which was located in an area of mature karst development, virtually no reflections were re-

Figure 11. Stack (nonmigrated) of VTVC Line SH1.: SH-wave line acquired on carbonate rocks on the crest of the Bane Dome. Note reflections at 2.8-3.2 s characteristic of the Cambrian sequence. Variability of data quality interpreted to be caused by local karst effects.

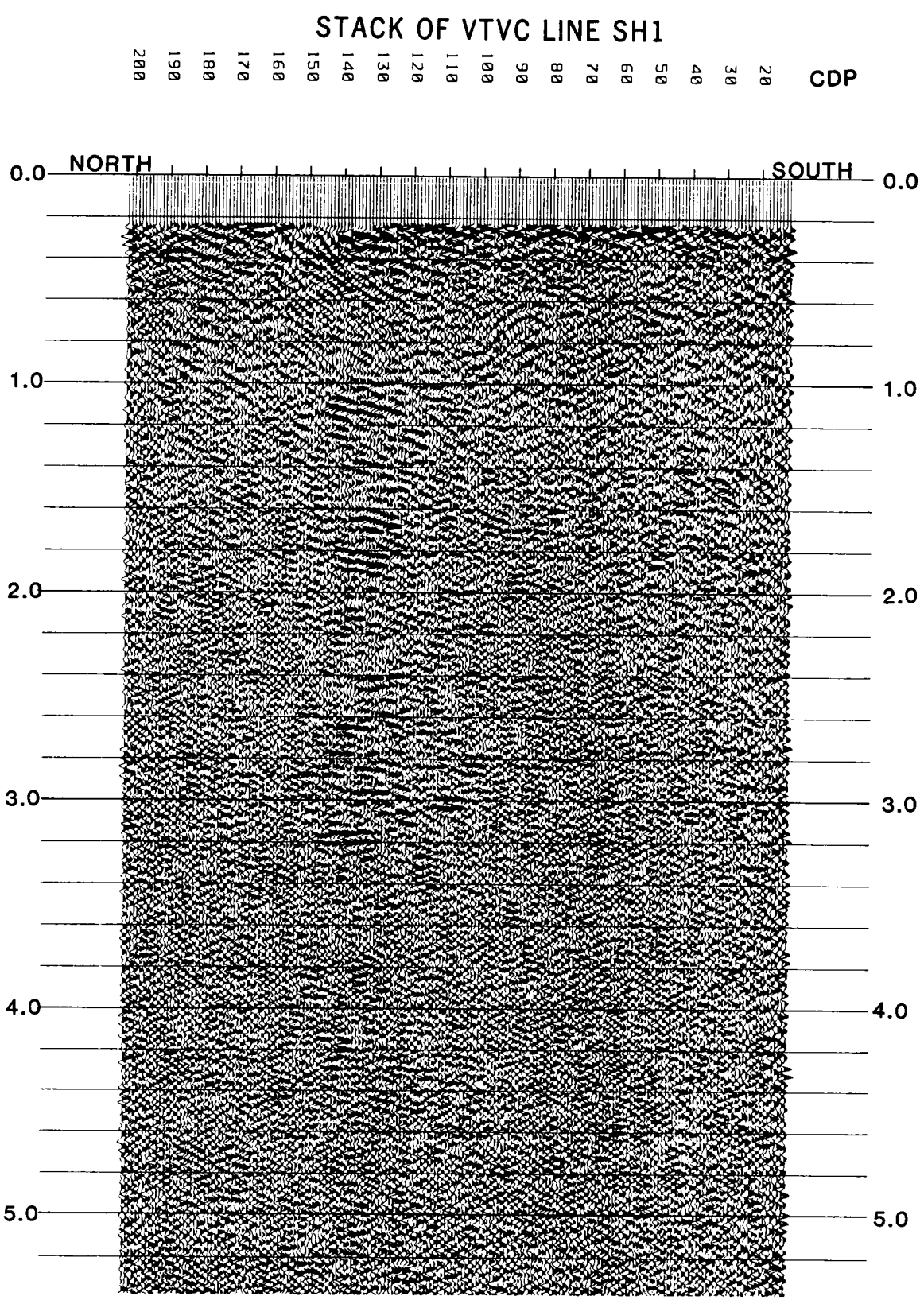
STACK OF VTVC LINE SH1
200
190
180
170
160
150
140
130
120
110
100
90
80
70
60
50
40
30
20
CDP
NORTH
SOUTH
0.0
1.0
2.0
3.0
4.0
5.0

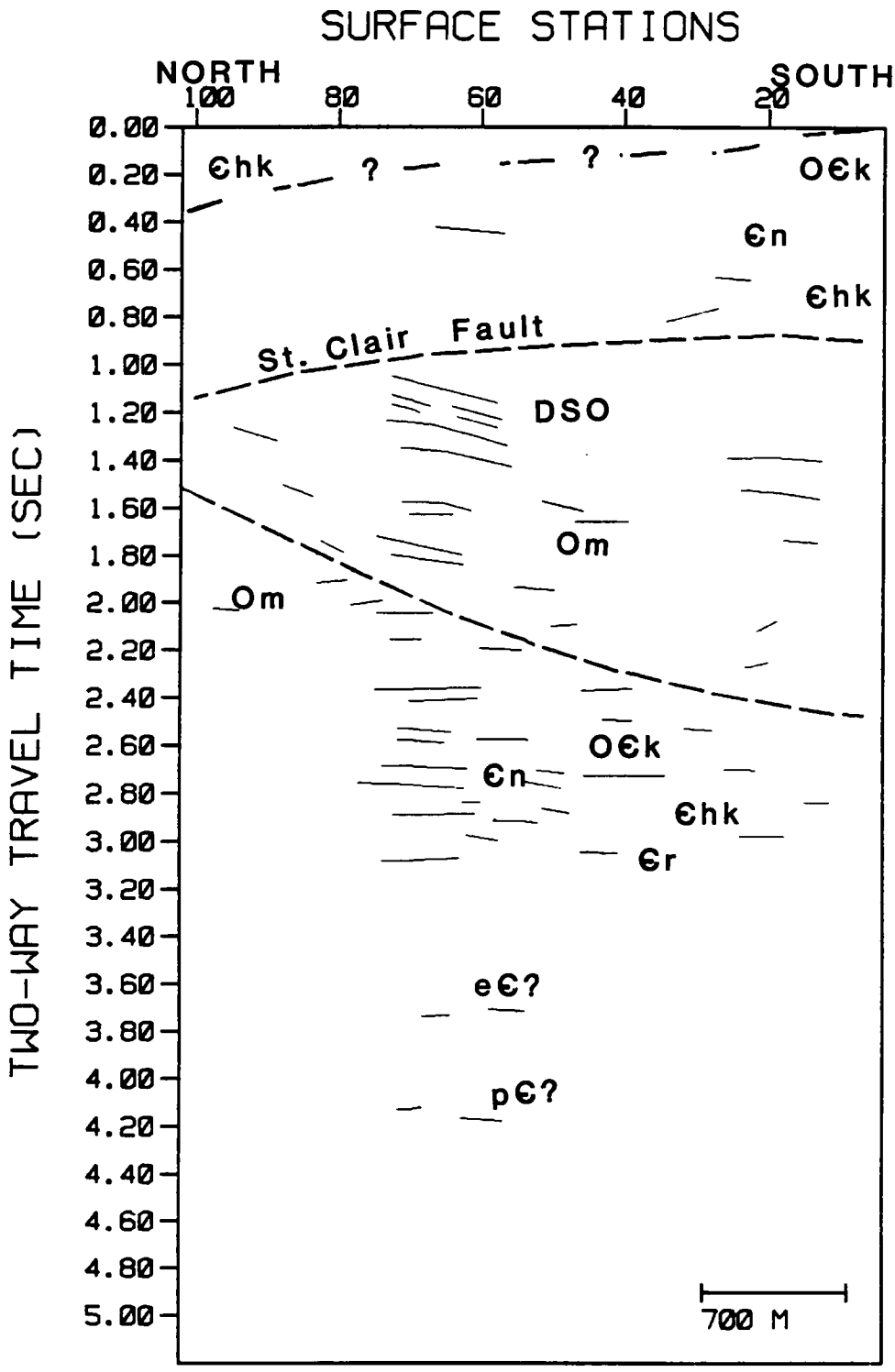

Figure 12. Interpretation of VTVC Line SH1.: Autochthonous Cambrian sequence interpreted at 2.8-3.2 s. Interpreted horse blocks "a" and "b" supporting the Bane Dome.

corded. Data from Line SH3 was also affected by localized karst, but not to the extent of Line SH4.

In general, approximately 50 percent of the SH-wave data acquired over areas underlain by carbonates was deemed acceptable in its final stacked form. This compares favorably to the P-wave results in which 100 percent of the P-wave data in this area can be considered unacceptable.

As previously mentioned, also included in this study are two seismic lines acquired by Virginia Tech in 1981 for the Virginia Division of Mineral Resources. These lines were located in the southern portion of the study area (Figure 2). The northern portions of both lines lie on the southern exposed portion of the Saltville thrust sheet. Both linfs continue to the south onto the Pulaski thrust sheet. These lines were acquired for the purpose of subsurface mapping of the coal units in the Mississippian Price Formation within the Saltville thrust sheet. A stack of Line VDMR1 is shown in Figure 13. Note the excellent data quality in the northern portion of the line where data were acquired while on the clastic rocks of the Saltville thrust sheet. However, data quality rapidly declines where the line moves onto the Pulaski thrust sheet. This example of data quality loss is typical in this area when P-wave data is acquired over carbonate rocks. In the southern portion of the line, the rocks at the surface are again clastics of the Saltville thrust sheet, therefore, data quality improves.

Projecting the surface geology into the subsurface and using the seismic stratigraphic relationships previously discussed, an interpretation of Line VDMR1 is shown in Figure 14. Of interest is the nature of

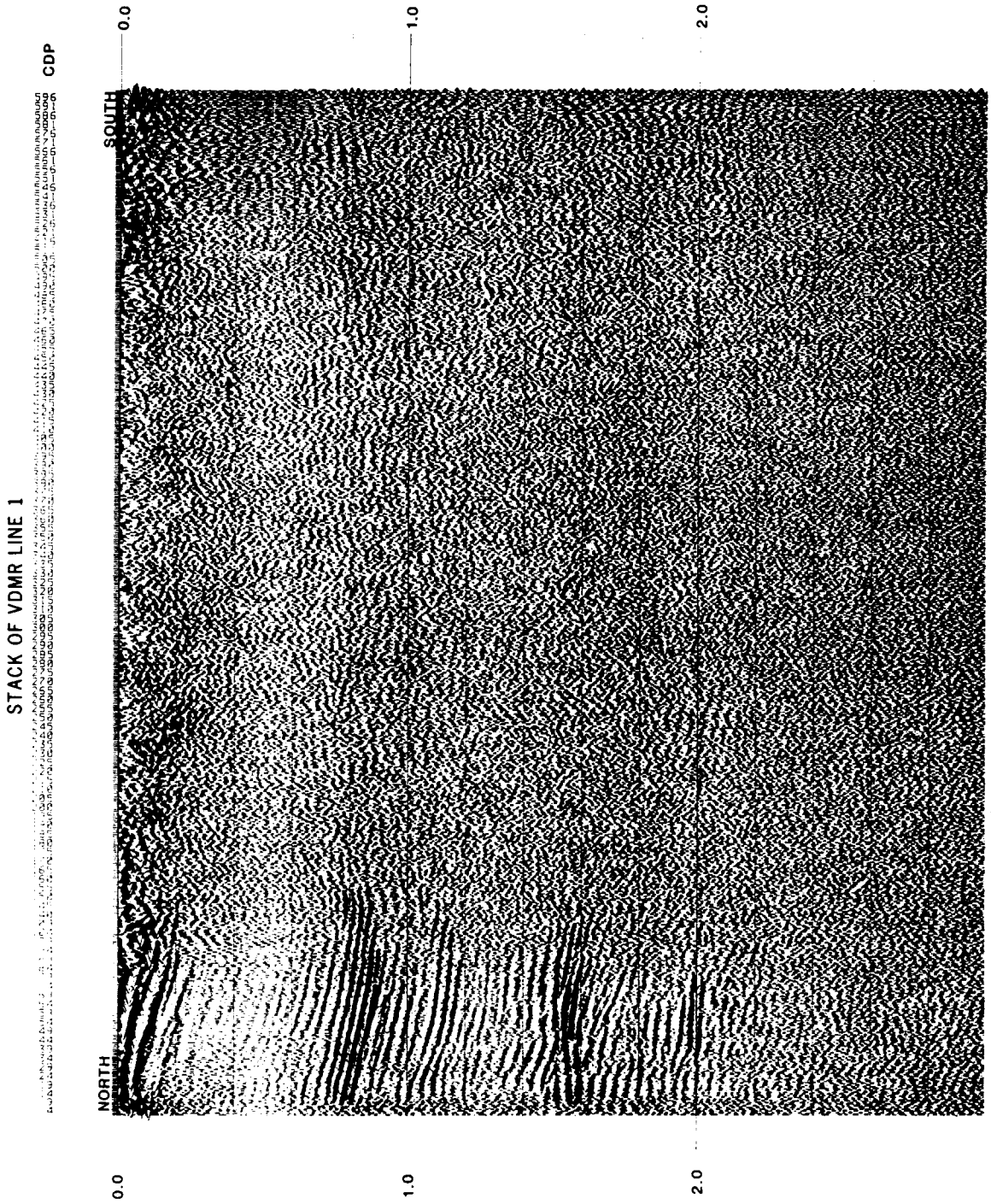

Figure 13. Stack (nonmigrated) of Line VDMR1.: P-wave line acquired over both clastic carbonate rocks. Note degradation of data where source and receivers are located on carbonate rocks.

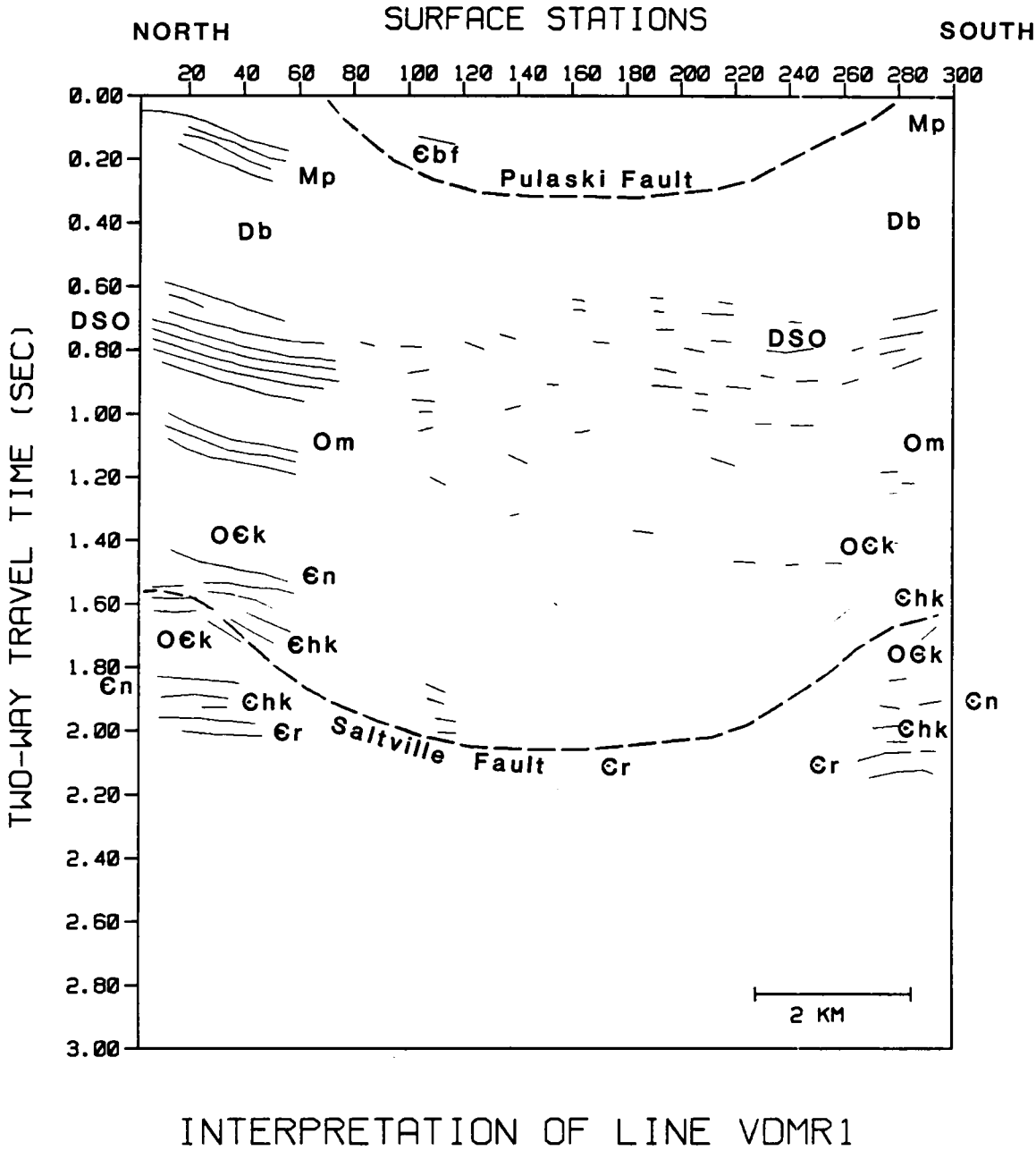

Figure 14. Interpretation of Line VDMR1.: Northern portion of line, where the line was acquired over clastic rocks of the Saltville thrust sheet has good data quality. Thrust sheet continues under the Pulaski thrust sheet and is then exposed in Price Mountain window. Ramps developed in footwall blocks of the Cambro-Ordovician sequence.

the Saltville thrust sheet, which underlies the Pulaski thrust sheet and is then exposed again at the surface in the Price Mountain Anticline.

The structural feature most evident is the ramp structure in the northern portion of the line, where the basal thrust which had been based in the shales of the Ordovician (probably the Mocassin Formation), now cuts through the Lower Ordovician and Cambrian units to become a basal thrust within the Rome Shale. This occurs again in the southern portion of the line under the Price Mountain Anticline, but is not as evident on this portion of the section. The autochthonous Cambro-Ordovician sequence beneath Price Mountain is also substantiated by a dynamite-source reflection study centered on the crest of Price Mountain by Kolich (1974). The characteristic reflection signature of the Nolichucky and Rome formational contacts were noted at the same approximate depth as interpreted on Line VDMR1.

The unusual nature of the basal thrust in the Rome which ramps both upward in the northern portion of the line and downward in the southern portion of the line is due to the fact that this line was not acquired perfectly along the dip of the rock units. It is interpreted that Line VDMR1 cuts obliquely across a frontal ramp (northern portion) and a lateral ramp (southern portion), yielding this unusual apparent structure.

As was previously mentioned, VTVC Line 1 was sited on the Devonian clastic sequence within the Saltville thrust sheet. A final stack (non-migrated) of VTVC Line 1, after crossdip removal (CDR), is shown in Figure 15. An interpretation of Line 1, based predominantly on the projection of surface geology into the subsurface and supported by Line VDMR1, is shown in Figure 16. Note the interpreted depth of the Saltville

Fault and its relationship with the previous mentioned crossdip effects. The trailing edge of the St. Clair Fault is interpreted as existing under this line with only the Cambro-Ordovician units within the sheet in this area. The St. Clair sheet then overlies a frontal ramp developed within the autochthonous Cambro-Ordovician sequence.

Geologic Interpretation

There have been three previously published cross-sections through the Bane Dome (Cooper, 1968; Milici, 1970; Perry et al., 1979). The first cross section (Cooper, 1961) was constructed assuming basement involvement and will not be discussed in detail in this text. The cross sections constructed by the latter authors (Milici, 1970 and Perry et al., 1979) are shown in Figure 17. These cross sections are consistent with the thin-skinned tectonic style of the Appalachians and exhibit the evolution of the structural interpretation of this complex area as new data became available.

A series of cross sections, based on the Virginia Tech reflection seismic data and constrained by the surface geology and borehole information, are shown in Figure 18 to Figure 20. They are in part modified from previous work by Perry et al., (1979), Schultz (1983) and Bartholemew and Lowery (1979). Fault blocks "a" and "b" are similar to those discussed by Perry et al., (1979) in apparent structural style, but lithologies and lateral extent are radically different.

Starting at the northern portions of the cross sections, there are a number of features which are worth noting. The structural style of the

Figure 15. Stack (nonmigrated) of VTVC Line 1.: P-wave strike line acquired over a clastic sequence within the Saltville thrust sheet. Stack section has had crossdip removal (CDR) applied.

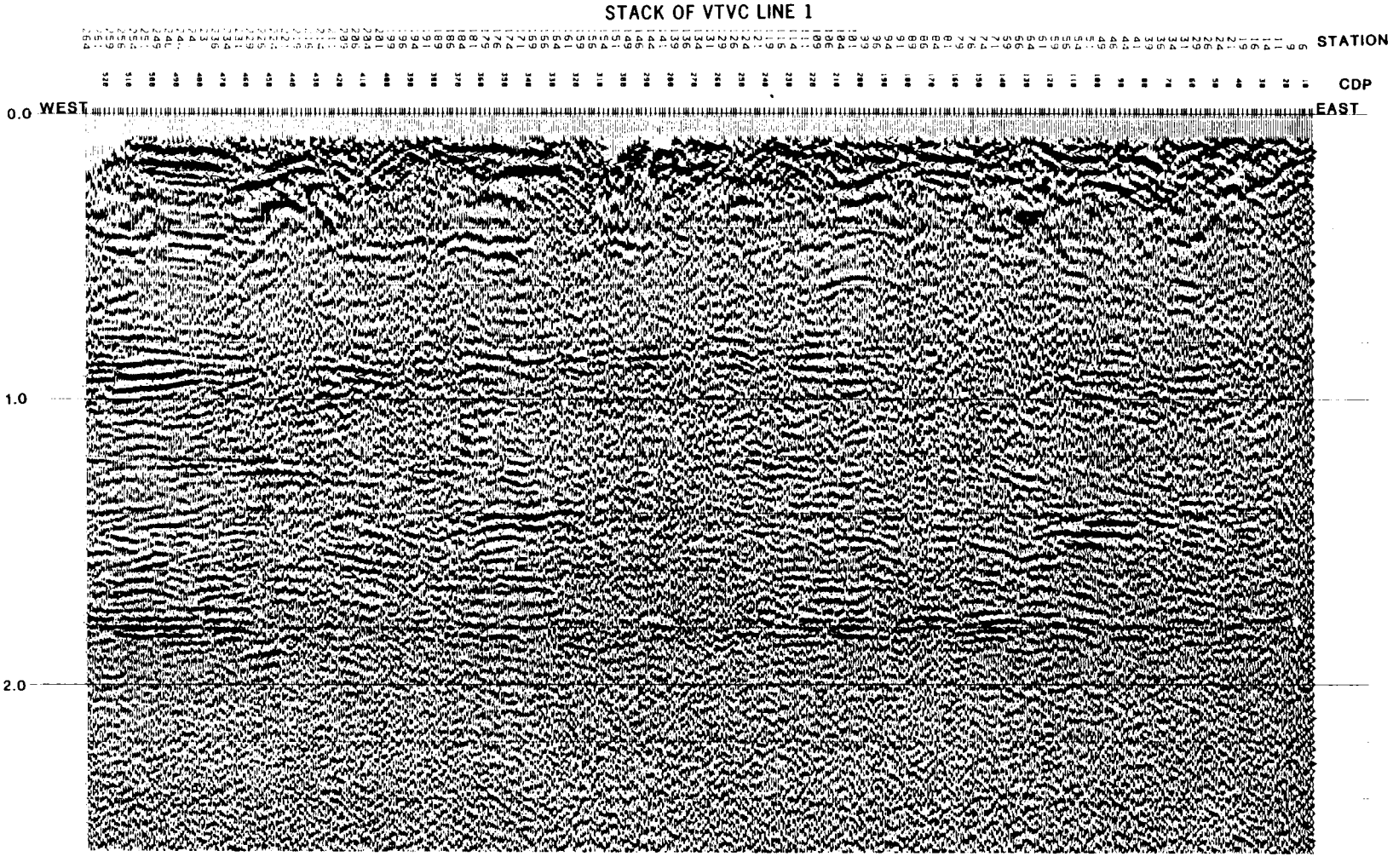
STACK OF VTVC LINE 1
STATION
CDP
0.0
WEST
EAST
1.0
2.0

Figure 16. Interpretation of VTVC Line 1.: Interpretation based on surface geology and seismic tie lines (VDMR1) and stratigraphic relationships determined from adjacent areas. Lower portion (Cambrian to Silurian) of the Saltville thrust sheet passes through the section, as well as the trailing edge of the hanging wall of the St. Clair thrust sheet. Ramp is developed within the Cambrian Honaker Formation.

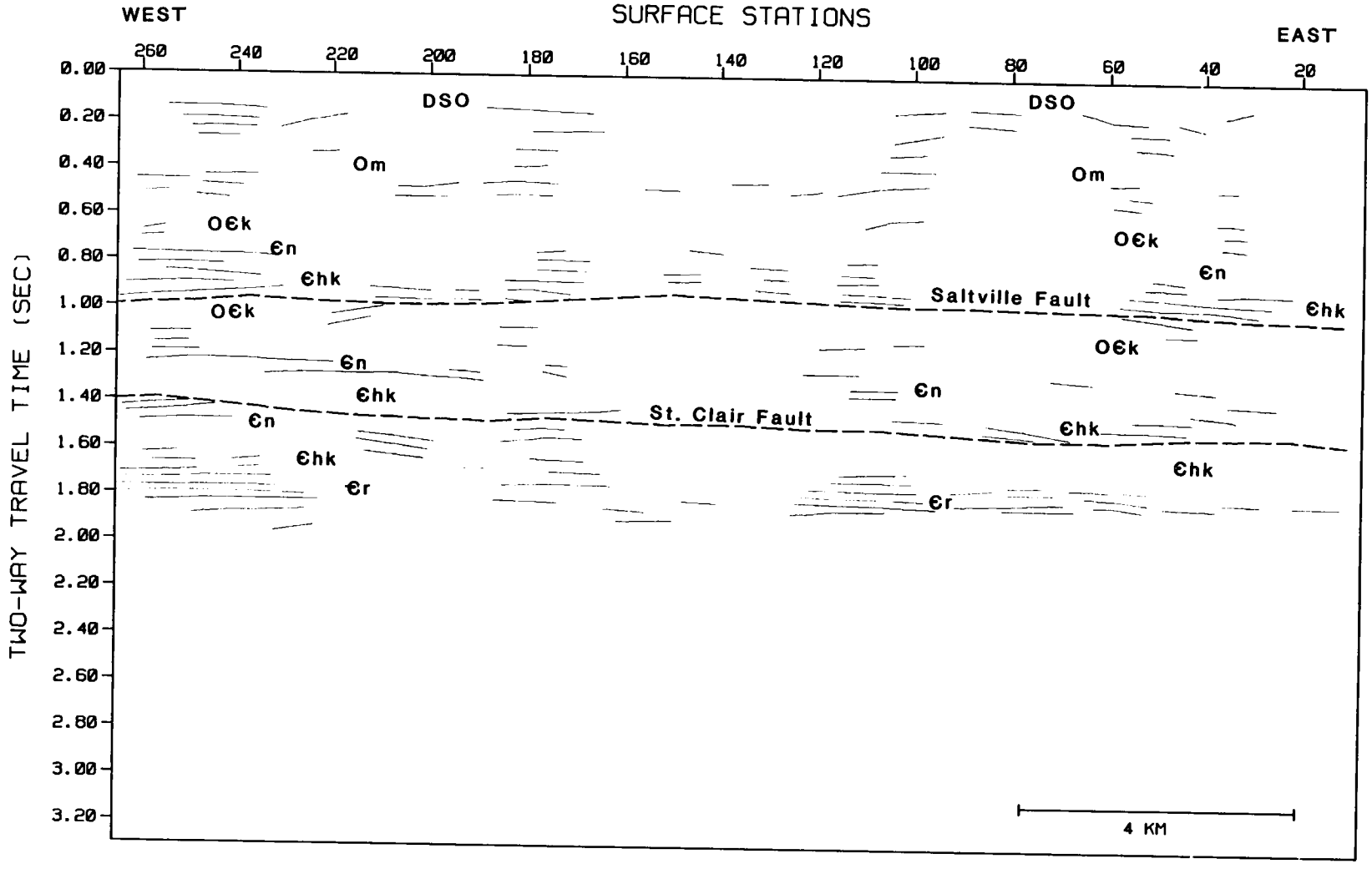

INTERPRETATION OF VTVC LINE1

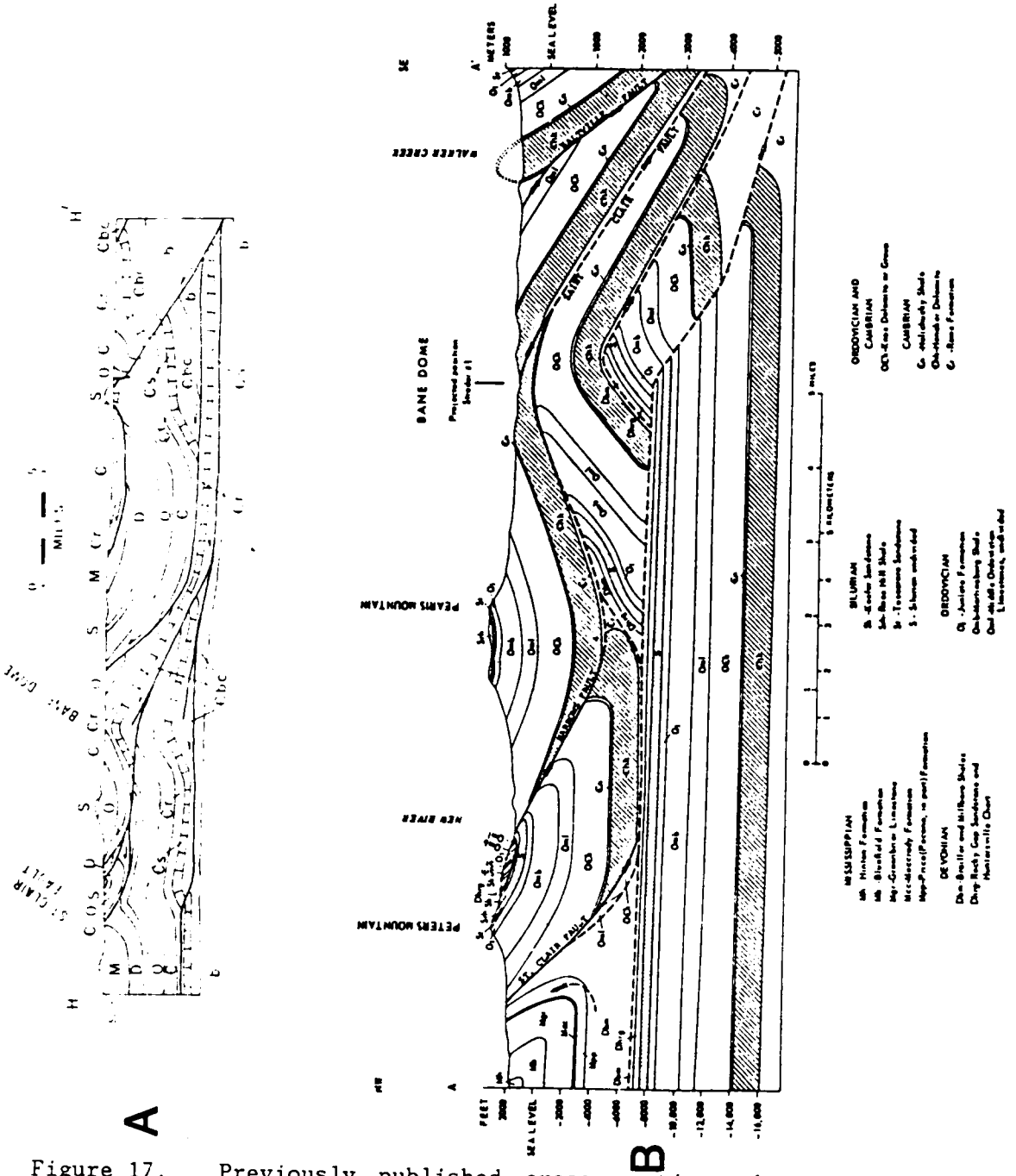

Figure 17. Previously published cross sections through the Bane Dome: A) Cross section constructed by Milici, 1970 through the Bane Dome constrained by surface geology. B) Cross section constructed by Perry et al., 1979 through the Bane Dome area, constrained by surface geology, and published gravity data (Sears and Robinson, 1971).

Figure 18. Cross section A-A' through the area of study: Cross section incorporates interpretations of seismic sections as noted, pertinent and available borehole data. Portions of cross sections are modified from Perry et al., (1979), Schultz (1983), and Bartholemew and Lowry (1979).

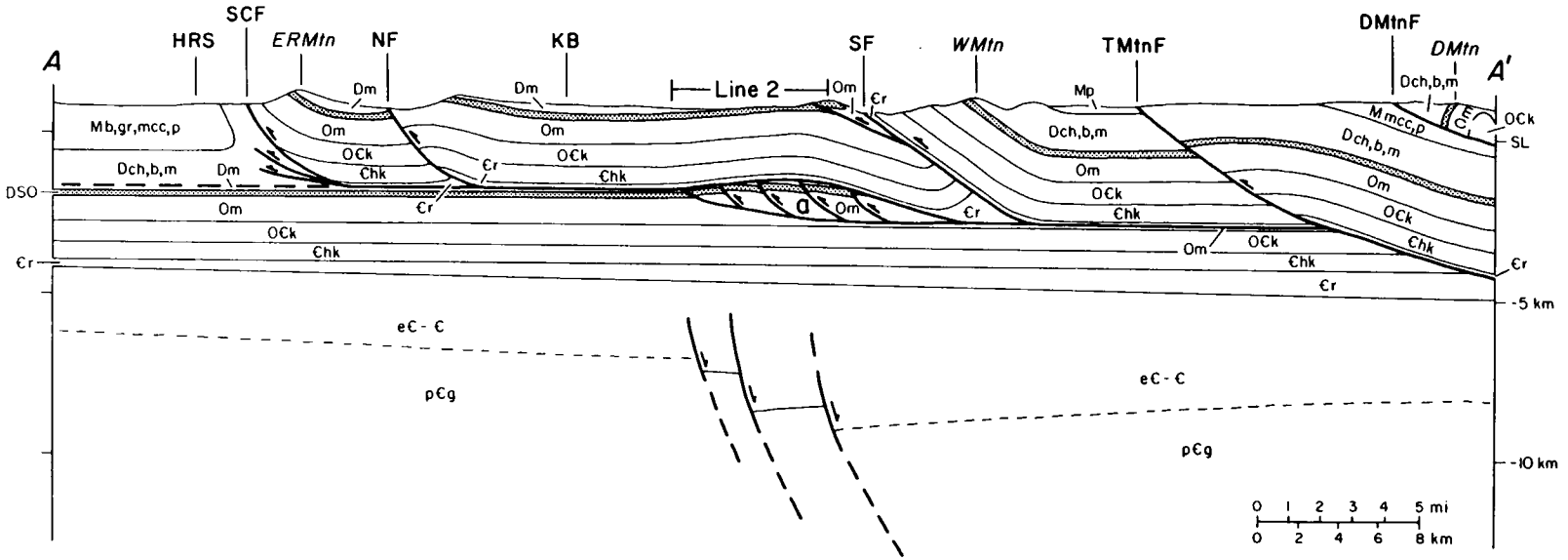

EXPLANATION

FAULTS

- thrust faults, dashed where inferred
- normal faults, dashed where inferred
- contacts, dashed where inferred

SEISMIC LINES

- ⊢Line 2⊣ in plane of section
- ⊗ perpendicular to plane of section

EARTHQUAKE HYPOCENTERS

- O ERZ > 5 km
- ● ERZ < 5 km

- borehole
- a, b horseblocks as referred to in text

GEOGRAPHIC FEATURES

- *ERMtn* East River Mtn.
- *PMtn* Peters Mtn.
- *WMtn* Walker Mtn.
- *DMtn* Draper Mtn.

GEOLOGICAL FEATURES

- HRS Hurricane Ridge Syncline
- SCF St Clair Fault
- NF Narrows Fault
- KB Kimberling Basin
- BD Bane Dome
- SF Saltville Fault
- TMtnF Tract Mtn. Fault
- DMtnF Draper Mtn Fault
- PF Pulaski Fault
- BF Blacksburg Fault

STRATIGRAPHY

Mississippian
Mb,gr,mcc,p — Mb, Bluefield Formation; Mgr, Greenbrior Formation; Mmcc, McCrady Formation; Mp, Price Formation

Devonian
Dch,b,m — Dch, Chemung Formation; Db, Brallier Shale; Dm, Millboro Shale

Devonian-Silurian-Ordovician
DSO — Lower Devonian, Silurian and Upper Ordovician Sequence. includes Silurian Rose Hill and Tuscarora Formations and Ordovician Juniata Formation

Ordovician
Om — Martinsburg and Moccasin Formations and Middle Ordovician undivided limestones

Cambro-Ordovician
OCk — Knox Group

Cambrian
Chk — Honaker Dolomite: includes Nolichucky Shale

Cr — Rome Shale

Precambrian-Cambrian
eC-C — Eocambrian-Cambrian undivided sediments

pCg — Grenville basement

Pulaski Thrust Sheet

Cambrian
Cc — Conococheague Formation

Ce — Elbrook Formation

Cbf — Broken Formation (Elbrook, Rome and breccia)

Figure 19. Cross section B-B' through the area of study: Cross section incorporates interpretations of seismic sections as noted, pertinent and available borehole data. Portions of cross sections are modifies from Perry et al., (1979), Schultz (1983), and Bartholemew and Lowry (1979).

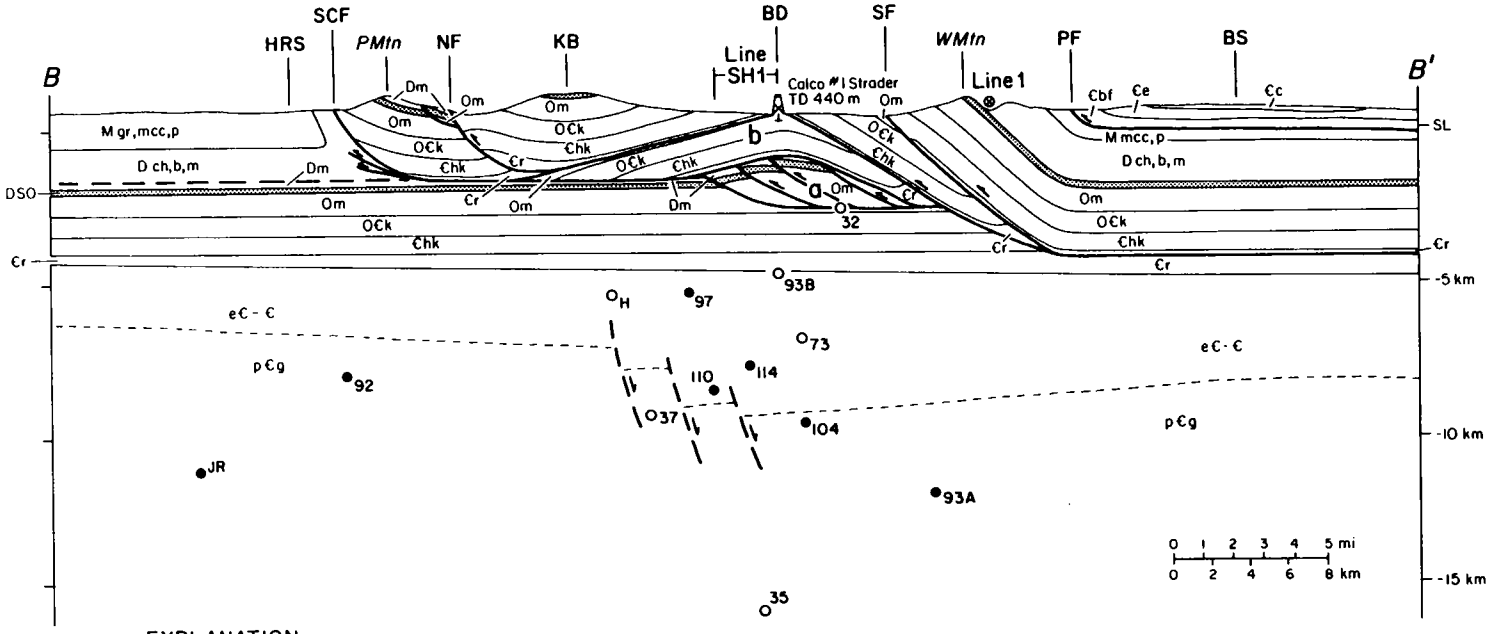

EXPLANATION

FAULTS

thrust faults, dashed where inferred

normal faults, dashed where inferred

contacts, dashed where inferred

SEISMIC LINES

Line 2 — in plane of section

⊗ perpendicular to plane of section

EARTHQUAKE HYPOCENTERS

○ ERZ > 5 km

● ERZ < 5 km

borehole

a, b horseblocks as referred to in text

GEOGRAPHIC FEATURES

ERMtn	East River Mtn
PMtn	Peters Mtn.
WMtn	Walker Mtn
DMtn	Draper Mtn

GEOLOGICAL FEATURES

HRS	Hurricane Ridge Syncline
SCF	St Clair Fault
NF	Narrows Fault
KB	Kimberling Basin
BD	Bane Dome
SF	Saltville Fault
TMtnF	Tract Mtn. Fault
DMtnF	Draper Mtn. Fault
PF	Pulaski Fault
BF	Blacksburg Fault

STRATIGRAPHY

Mississippian
M b,gr,mcc,p — Mb, Bluefield Formation, Mgr, Greenbriar Formation; Mmcc, McCrady Formation; Mp, Price Formation

Devonian
D ch,b,m — Dch, Chemung Formation; Db, Brallier Shale; Dm, Millboro Shale

Devonian-Silurian-Ordovician
DSO — Lower Devonian, Silurian and Upper Ordovician Sequence. includes Silurian Rose Hill and Tuscarora Formations and Ordovician Juniata Formation

Ordovician
Om — Martinsburg and Moccasin Formations and Middle Ordovician undivided limestones

Cambro-Ordovician
OCk — Knox Group

Cambrian
Chk — Honaker Dolomite: includes Nolichucky Shale

Cr — Rome Shale

Precambrian-Cambrian
eC-C — Eocambrian-Cambrian undivided sediments

pCg — Grenville basement

Pulaski Thrust Sheet

Cambrian
Cc — Conococheague Formation

Ce — Elbrook Formation

Cbf — Broken Formation (Elbrook, Rome and breccia)

Figure 20. Cross section C-C' through the area of study: Cross section incorporates interpretations of seismic sections as noted, pertinent and available borehole data. Portions of cross sections are modified from Perry et al., (1979), Schultz (1983), and Bartholemew and Lowry (1979).

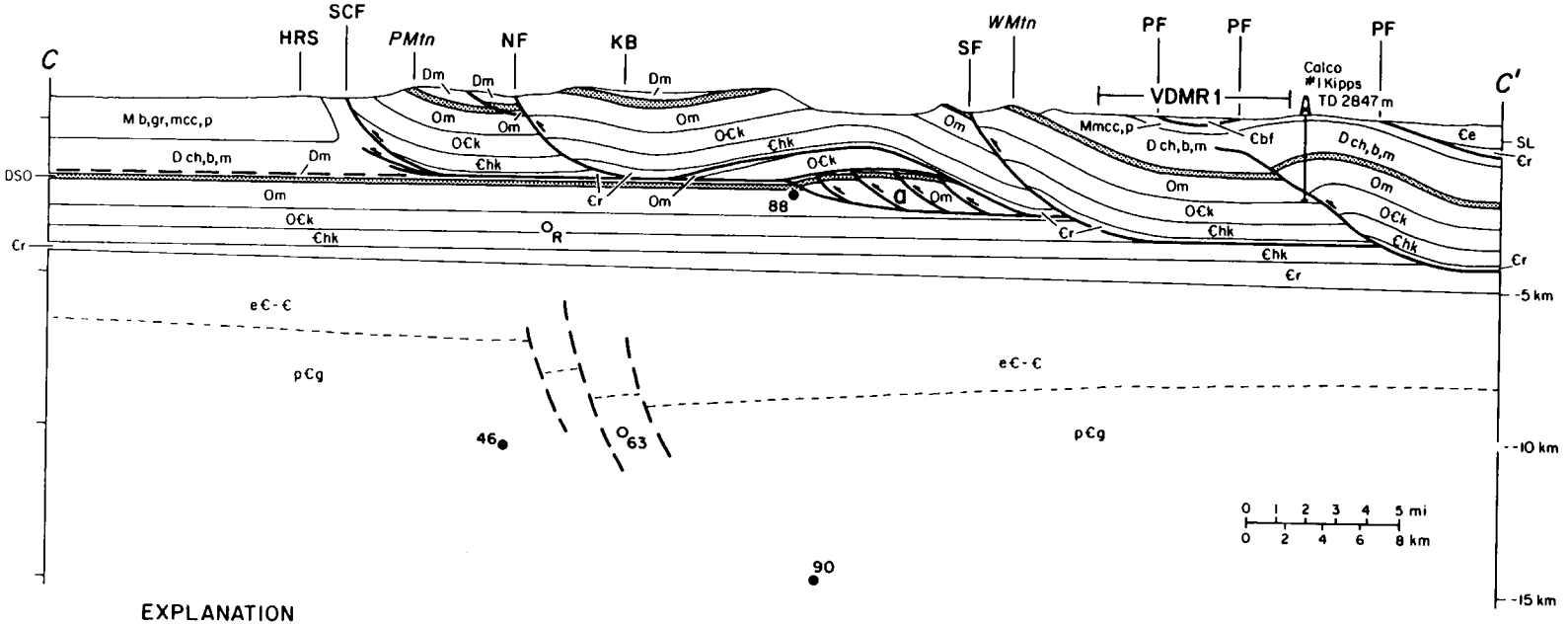

EXPLANATION

FAULTS

- thrust faults, dashed where inferred
- normal faults, dashed where inferred
- contacts, dashed where inferred

SEISMIC LINES

- Line 2 — in plane of section
- ⊗ perpendicular to plane of section

EARTHQUAKE HYPOCENTERS

- O ERZ > 5 km
- ● ERZ < 5 km

- borehole
- a, b horseblocks as referred to in text

GEOGRAPHIC FEATURES

ERMtn	East River Mtn
PMtn	Peters Mtn
WMtn	Walker Mtn
DMtn	Draper Mtn

GEOLOGICAL FEATURES

HRS	Hurricane Ridge Syncline
SCF	St Clair Fault
NF	Narrows Fault
KB	Kimberling Basin
BD	Bane Dome
SF	Saltville Fault
TMtnF	Tract Mtn. Fault
DMtnF	Draper Mtn Fault
PF	Pulaski Fault
BF	Blacksburg Fault

STRATIGRAPHY

Mississippian
M b,gr,mcc,p — Mb, Bluefield Formation; Mgr, Greenbriar Formation; Mmcc, McCrady Formation, Mp, Price Formation

Devonian
D ch,b,m — Dch, Chemung Formation; Db, Brallier Shale; Dm, Millboro Shale

Devonian-Silurian-Ordovician
DSO — Lower Devonian, Silurian and Upper Ordovician Sequence: includes Silurian Rose Hill and Tuscarora Formations and Ordovician Juniata Formation

Ordovician
Om — Martinsburg and Moccasin Formations and Middle Ordovician undivided limestones

Cambro-Ordovician
OCk — Knox Group

Cambrian
Chk — Honaker Dolomite: includes Nolichucky Shale
Cr — Rome Shale

Precambrian-Cambrian
eC-C — Eocambrian-Cambrian undivided sediments
pCg — Grenville basement

Pulaski Thrust Sheet

Cambrian
Cc — Conococheague Formation
Ce — Elbrook Formation
Cbf — Broken Formation (Elbrook, Rome and breccia)

Appalachian front is well documented from surface geology. The flat lying rocks of the Appalachian Plateau are abruptly folded at the Appalachian front into a tight, overturned syncline (Hurricane Ridge Syncline). The first thrust fault to the south is the St. Clair Fault. As with most faults in this area, the rocks exposed at the leading edge of the fault are the Cambro-Ordovician sequence. Rocks from the Cambrian to the DSO sequence are exposed within the St. Clair thrust sheet. From the cross sections, the displacement along the St. Clair Fault at the northeastern portion of the study area is approximately 30 km. From surface geology, the St. Clair Fault decreases in offset and dies out approximately 50 km northeast of the study area.

The next major fault to the south is the Narrows Fault. This fault which is exposed for hundreds of kilometers to the south, decreases in offset toward the north and subsequently dies out in the northeastern portion of the study area. From this and the constraints by the interpretation of Line 2, the Narrows Fault is interpreted as a break-back imbricate fault of the major thrust fault in this area, the St. Clair Fault.

To the south, the rocks of the St. Clair-Narrows thrust sheet are folded into two structures which have been previously mentioned; the Kimberling Basin and the Bane Dome. It is interpreted that the Bane Dome is supported by two horse blocks, "a" and "b" . From seismic data, specifically Line 2, it is interpreted that horse block "b" has a limited lateral extent, and is found only in an area directly under the Bane Dome. Conversely, block "a" is interpreted to have a greater lateral extent

which extends along the length of this study area and continues along strike toward the northeast and southwest.

South of the Kimberling Basin and the Bane Dome, is the leading edge of the Saltville thrust sheet. This major thrust sheet has rocks from Cambrian to Mississippian exposed along its length. Note the decrease in throw along the length of the Saltville Fault as the cross sections progress to the northeast. This is consistent with surface geology which suggests that the Saltville Fault dies out approximately 15 km to the northeast of the area of study.

Farther to the south is the Pulaski Fault. The unusual outcrop pattern of this fault can be seen in Figure 2. It is interpreted that the Pulaski Fault overlies the complete Saltville thrust sheet. This is supported by Line VDMR1 and the exposure of Mississippian rocks in the Price Mountain Window. It is interpreted that the unsual shape of the Pulaski Fault is caused by the draping of the Saltville and Pulaski thrust sheets into the volume previously containing horse block "b" . The interpretation of this and related features in this area are shown in a pair of block diagrams (Figure 21). From the surface geology and the subsurface geophysics, horse block "b" is interpreted to have been formed by failure of the footwall block during thrusting of the St. Clair Fault. This block was caught up in thrusting movement that generated approximately 30 km of displacement along the St. Clair Fault, moving block "b" into its present position. The absence of horse block "b" resulted in a "hole" and folding in the overlying Saltville and Pulaski thrust sheets. Erosion of these sheets then resulted in the unusual surface pattern of the Pulaski Fault in the study area (Figure 21).

Figure 21. Block diagrams based on previous cross sections: A) Shows relationship between footwall geometry and horse structures. B) Geologic model of study area in block diagram form.

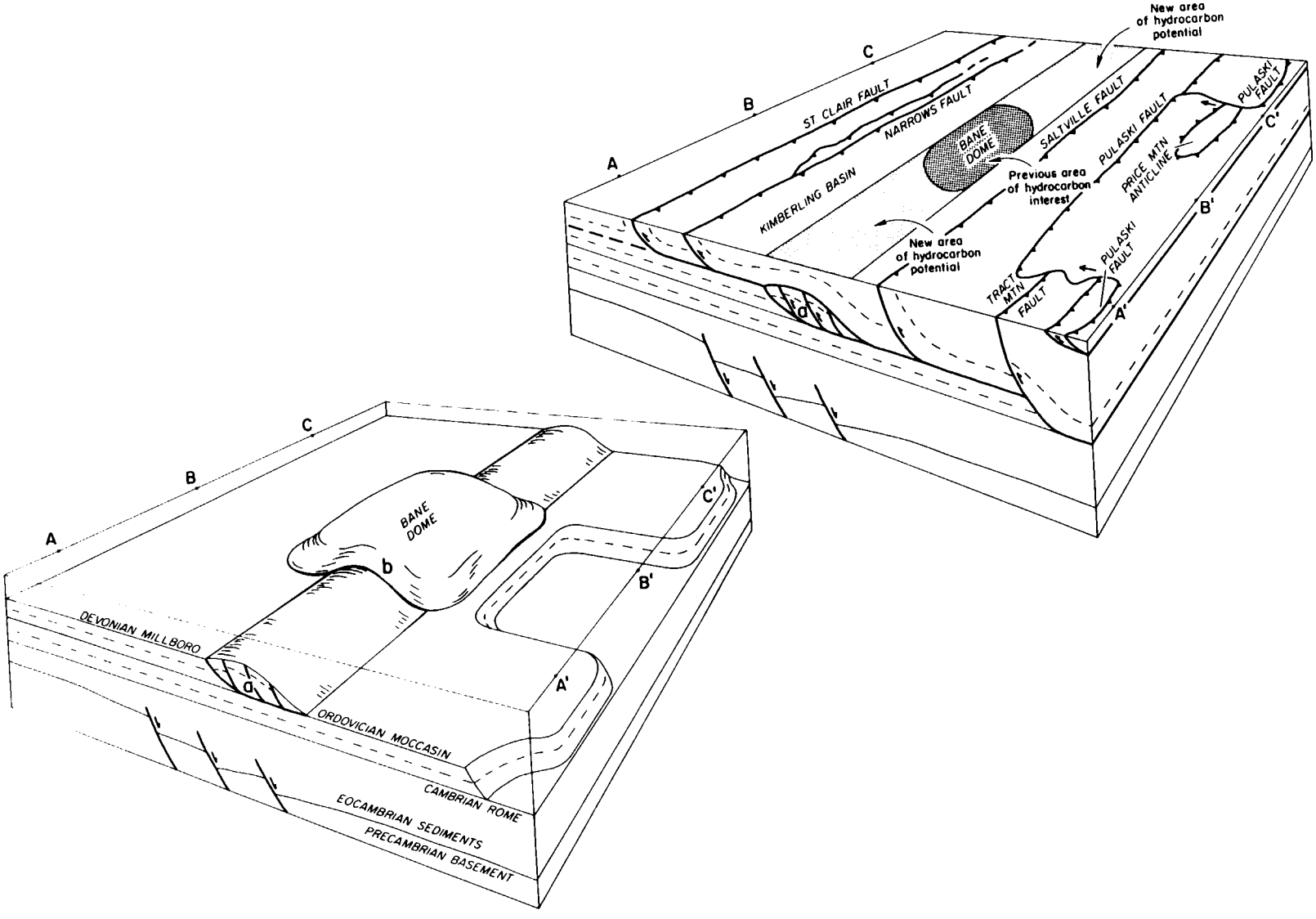
New area
of hydrocarbon
potential
A
B
C
ST CLAIR FAULT
NARROWS FAULT
KIMBERLING BASIN
BANE
DOME
SALTVILLE FAULT
PULASKI FAULT
PULASKI
FAULT
C'
Previous area
of hydrocarbon
interest
PRICE MTN
ANTICLINE
B'
New area
of hydrocarbon
potential
TRACT
MTN
FAULT
PULASKI
FAULT
A'
a
A
B
C
BANE
DOME
b
C'
B'
DEVONIAN MILLBORO
a
A'
ORDOVICIAN MOCCASIN
CAMBRIAN ROME
EOCAMBRIAN SEDIMENTS
PRECAMBRIAN BASEMENT

Horse block "a" is interpreted as being the last feature formed during the thrusting of the Alleghenian orogeny in this region. It was also formed by footwall failure, but its offset is small in comparison to horse "b" .

A reconnaissance gravity survey was compiled in the Bane Dome area by Sears and Robinson (1971). A density model of cross section B-B' and a comparison of the observed and calculated gravity profile along the cross section is shown in Figure 22. Observed gravity data were acquired from contoured values of residual Bouguer anomaly along the length of the geologic cross section. The observed gravity values have a scatter of ± 1 mgal within 5 km along strike of the observed profile. The calculated gravity values were determined by assuming a two-dimensional model with density variations consistent with Sears and Robinson (1971), Edsall (1974) and Kolich (1974). Values for each point along the profile were calculated by summing the gravitational attraction of each two-dimensional body at that point. The results demonstrate that the geologic model is consistent with the observed gravity.

In summary, the Bane Dome is interpreted as a duplex structure, supported by two horse blocks, each of which contains distinct lithologies but that were formed under similar conditions. Block "b" was transported approximately 30 km during the thrusting of the St. Clair-Narrows thrust sheet. Block "a" probably was formed during the emplacement of block "b" beneath what is now known as the Bane Dome.

Block "a" might be the feature of most economic interest, containing both possible source and reservoir rocks (Silurian Tuscarora and Rose Hill Formations, and Devonian and Ordovician sandstones and shales). The

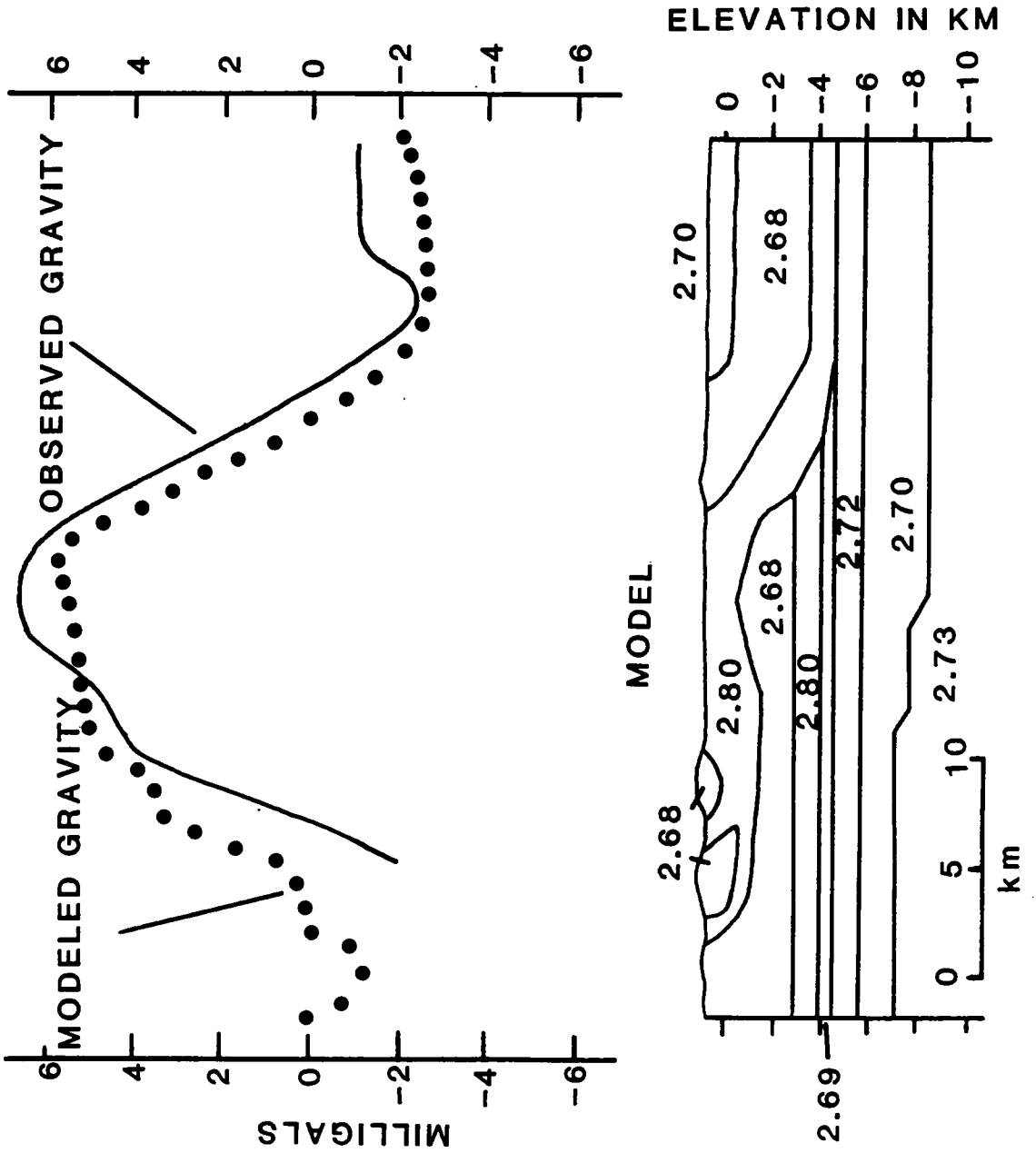

Figure 22. Observed and calculated gravity profiles over the Bane Dome: Observed gravity values from Sears and Robinson, 1971 compared to density model of cross section B-B' constructed from reflection seismic data and surface geology. Density values from Sears and Robinson (1971).

general structure of block "a" is anticlinal with internal minor thrusting that might have introduced increased porosity and permeability. The lateral extent of this structure (estimated at greater than 100 km) as well as the lithologies within the horse make this structure more interesting for hydrocarbon exploration than the Bane Dome alone. A deeper test well located directly on the Bane Dome would test both horses within the duplex structure of the Bane Dome Complex.

Eocambrian rifting and present day seismicity

This area of the Appalachians is one where low intensity seismicity has been noted since the late 1880's. The local network of the Virginia Tech Seismological Observatory (including a World Wide Standard Seismic Network station, BLA) of 7 stations has been in operation since 1978. Twenty-four seismic events have been recorded in the area, defining a linear trend of epicenters. Locations and magnitudes of the events are listed in Appendix D, and shown in Figure 2.

Bollinger and Wheeler (1983) suggested that the earthquakes within the Giles County Seismic Zone might be generated along reactivated Eocambrian faults associated with a rifting event. This interpretation was based upon the depth and orientation of the events. The events occur at a depth which in general is deeper than the thickness of the Paleozoic sediments, while the general trend of the earthquakes are at an angle to the trend of structures apparent at the surface.

Interpretation of Line 2 (Figure 7 and Figure 8) suggests that there is a thickening of the units which lie below the autochthonous Cambrian

Rome Formation. It is interpreted that this thickening was caused by high angle normal faults active during the deposition of Late Precambrian-Early Cambrian (Eocambrian) sediments. Although these faults are evident only on Lines 2 and SH2, because of the trend of the seismic zone, it is inferred that they also underly the Bane Dome area where the reflection data are not of high enough quality to resolve these structures.

The location of these faults (based on the interpretation of Line 2) are shown in Figure 18. Fault locations on cross sections B-B' and C-C' are inferred by projecting the fault locations along the trend of the observed earthquakes. Additional seismic lines in the northern portion of the study area will be necessary to determine the exact orientation of these faults.

These faults are assumed to have originally formed during the opening of the proto-Atlantic Ocean (Iapteus), and were active up to the Early Cambrian. They became inactive before the deposition of the Rome Formation, evident from the absence of thickening of the Rome on Line 2. Disruption of the Cambro-Ordovician reflections evident in Figure 7 along the inferred trace of the faults probably defines a zone of increased fracturing of the surrounding rocks adjacent to the faults caused during reactivation. The faults trend approximately N 20-27°E (Munsey and Bollinger, 1984 and Munsey, 1984) and are being reactivated by the present compressional stress regime, causing a predominant strike-slip movement along the pre-existing faults.

DISCUSSION AND CONCLUSIONS

The results of Consortium years 1982-1984 can be summarized as follows:

1) Using a SH-wave Vibroseis source it was possible to acquire reflection seismic data in areas which previously have had a poor data history. In areas which had a minimum amount of karst present, SH-wave data acquired in areas underlain by carbonate rocks were far superior to P-wave data in that same environment. P-wave velocities, SH-wave velocities, and V_p/V_s ratios were useful for determining lithologies and stratigraphy in this geologically complex area with an absence of borehole information.

2) An accurate synthetic model was generated using geologic information derived from both laboratory and field evidence. This model was necessary to allow interpretation of the existing seismic lines in the absence of borehole information.

3) The velocity model determined by the P-wave and SH-wave Vibroseis studies agrees well with previous regional velocity data, especially V_p/V_s ratios.

4) A successful reflection seismic survey over an intraplate seismogenic zone identified faults which suggest a mechanism for the seismicity in the Appalachian Highlands of the eastern United States.

5) A detailed geologic interpretation was possible through the integration of reflection seismic data with surface geology. A series of

balanced cross sections were constructed which are consistent with the local gravity anomaly at the Bane Dome.

6) Identification of distinct horse blocks beneath the Bane Dome Complex increases greatly the area of hydrocarbon potential in an area which might be considered to be a rejuvenated "frontier" exploration area.

REFERENCES

Bartholemew, M. J. and Lowry, W. D., 1979, Geology of the Blacksburg Quadrangle, Virginia: Virginia Division of Mineral Resources Publication 14(GM81B), text and 1:24,000 scale map.

Bollinger, G. A. and Wheeler, R. L., 1983, The Giles County, Virginia, seismic zone, Science, **219**, 1063-1065.

Bollinger, G. A., Chapman, M. C., and Moore, T. P., 1980, Central Virginia Regional Seismic Network: Crustal velocity structure in central and southwestern Virginia; Prepared for U. S. Nuclear Regulatory Commission, Report no. NUREG/CR-1217, 187 p.

Butler, R. W. H., 1982, The terminology of structures in thrust belts; Journal of Structural Geology, **4**, 239-245.

Calver, J. L., 1963, Geologic map of Virginia: Virginia Div. Mineral Resources Geol. Map, Scale 1:500,000.

Cooper, B. N., 1961, Grand Appalachian excursion: Virginia Polytech. Inst. Eng. Expt. Sta. Ext. Ser. Geol. Guidebook 1, 187 p.

Cooper, B. N., 1964, Relation of stratigraphy to structure in the southern Appalachians, in Tectonics of the southern Appalachians: Virginia Polytech. Inst. Dept Geol. Sci. Mem. 1, 81-114.

Cooper, B. N., 1968, Profile of the folded Appalachians of western Virginia: Missouri Univ. Jour., no. 1, 27-64.

Edsall, R. W., 1974, A seismic reflection study over the Bane Anticline in Giles County, Virginia: M. S. thesis, Virginia Poly. Inst. and State Univ., Dept of Geol. Sciences, Blacksburg, 111 p.

Erickson, E. L., Miller, D. E., and Waters, K. H., 1968, Shear-wave recording using continuous signal methods: Part II - Later Experimentation, Geophysics, **33** , 240-254.

Fix, J. E., Robertson, J. D., and Pritchett, W. C., 1983, Shear-wave reflections in three West Texas basins with high-velocity surface rocks, Paper presented at the 53rd Annual International SEG Meeting, Las Vegas.

Gibson, B. and Larner, K., 1984, Predictive deconvolution and the zero-phase source, Geophysics, **49** , 379-397.

Kolich, T. M., 1974, Sesimic reflection and refraction studies in the Folded Valley and Ridge Province at Price Mountain, Montgomery

County, Virginia: Virginia Polytechnic Institute and State University, M. S. thesis, 139 p.

Larner, K. L., Gibson, B. R., Chambers, R., and Wiggins, R. A., 1979, Simultaneous estimation of residual static and crossdip corrections, Geophysics, **44** , 1175-1192.

McCormack, M. D., Dunbar, J. A., and Sharp, W. W., 1984, A case study of stratigraphic interpretation using shear and compressional seismic data, Geophysics, **49** , 509-520.

Milici, R. C., 1970, The Allegheny structural front in Tennessee and its regional tectonic implications, Am. Jour. Sci., **268**, 127-141.

Munsey, J. W. and Bollinger, G. A., 1984, Focal mechanisms for Giles County, Virginia and vicinity, (abs), Eqke. Notes, **56**, 8.

Munsey, J. W., 1984, Focal mechanism analysis for recent (1978-1984) Virginia earthquakes, Virginia Polytechnic Institute and State University: M. S. thesis, 214 p.

Perry, W. J., A. G. Harris, and L. D. Harris, 1979, Conodont-based reinterpretation of Bane Dome-Structural reevaluation of Allegheny frontal zone, Bull. Amer. Assoc. Pet. Geol., **63** , 647-654.

Ristow, D. and Jurczyk, D., 1975, Vibroseis deconvolution, Geophysical Prospecting, **23** , 363-379.

Schultz, A. P., 1983, Broken-Formations of the Pulaski Thrust Sheet near Pulaski, Virginia: Virginia Polytechnic Institute and State University, Ph.D. Disseration, 82 p.

Sears, C. E. and Robinson, E. S., 1971, Relations of Bouguer gravity anomalies to geologic structure in the New River District of Virginia; Geol. Soc. of Am. Bull. **82**, 2631-2638.

Stanley, C. B. and Schultz, A. P., 1983, Coal-bed methane resource evaluation Montgomery County, Virginia, Prepared for U. S. Department of Energy by the Virginia Division of Mineral Resources, 98 p.

APPENDIX A

Removal of Crossdip effects

For Line 1, software called Crossdip Removal (CDR) was developed and used by VTVC to remove the effects of crossdip. This correction projects reflection points into a plane that contains both the strike line and the normal incidence ray path. This method corrects for the time shift, ΔT, which is dependent upon the dip of the reflectors and the horizontal distance of the reflection point from a profile parallel to strike (Figure 23).

The first step in CDR is to resort each portion of the line with similar crossdip effects into common offset gathers. In the case of irregular shooting, common receiver gathers can also be used. Portions of the line must be small enough to insure that true structure is not removed. For this data, groups ranged from 30 to 50 CDPs per group with 35 m spacing between each CDP.

In common offset gathers, those reflections affected by crossdip have arrival times which are dependent on the depth and velocity of the units as well as the dip of the units and the deviation of the depth point from the strike line. These reflections will then appear to be dipping. Those reflections unaffected by crossdip will have arrival times which are dependent upon only the velocity and depth of the units. These reflections are characterized by their constant arrival times.

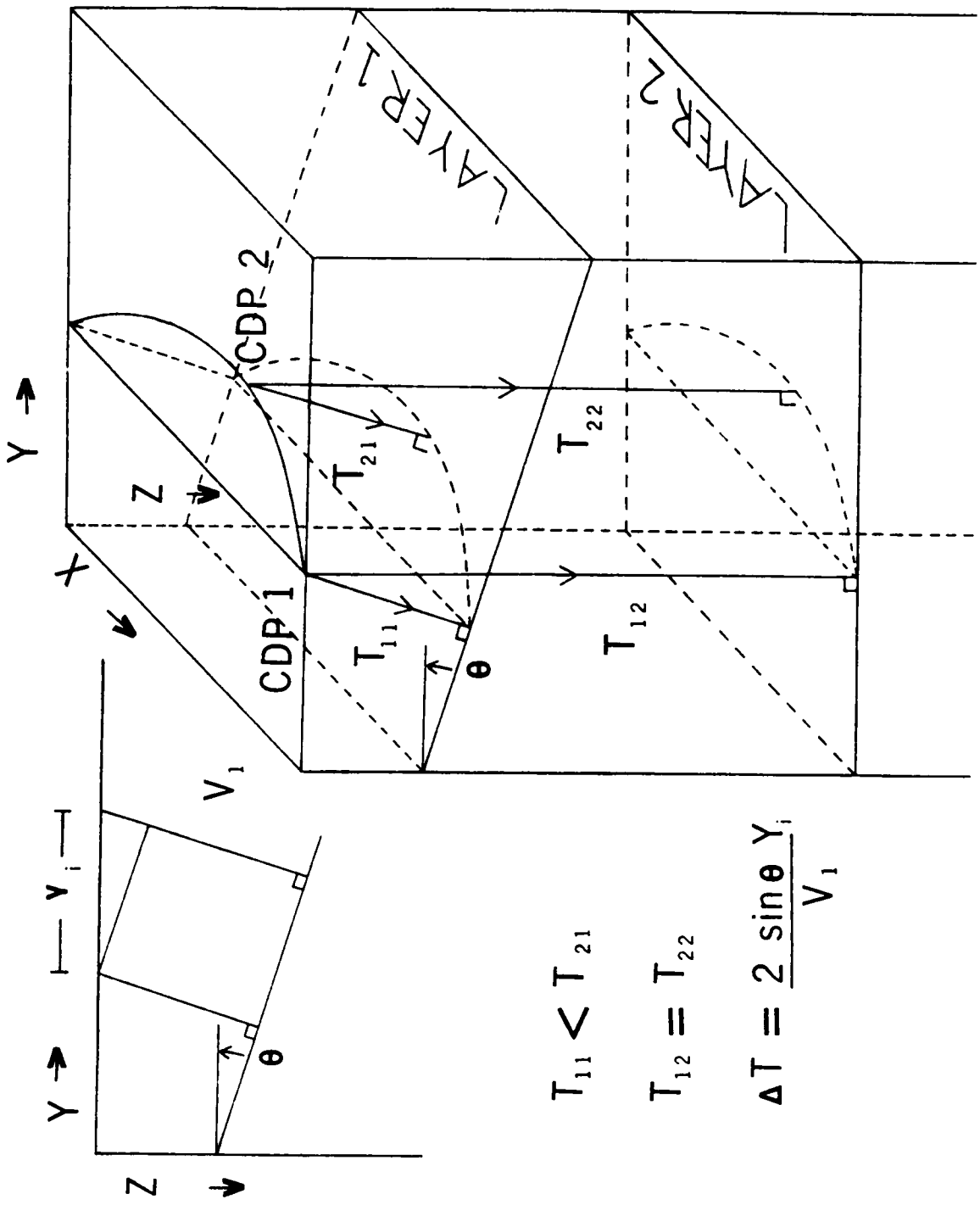

Figure 23. Definition of crossdip and its effect on stacked data.

Within the gathers, relative offsets are calculated for the distance between each receiver survey location. These offset values are necessary in calculating the dip of the reflections affected by crossdip. Semblance scans, similar to velocity spectrum analysis, are used to determine the values of ΔT as a function of horizontal distance and vertical travel-time for each trace. The effects of crossdip are then removed by applying the ΔT time shift over a given time range, in a method similar to removing normal moveout (NMO). Below that time range the trace is left unshifted.

Previous methods of crossdip analysis (e.g. Larner et al., 1979) allowed only static shifts to compensate for crossdip effects. CDR allows time variant shifts which remove the crossdip effects caused by a single or group dipping layers without disturbing those reflections in other portions of the trace unaffected by crossdip.

APPENDIX B

Minimum-phase Filter Deconvolution

An alternative to gapped deconvolution was first discussed by Ristow and Jurczyk (1979). They suggested using a minimum-phase filter on Vibroseis data to alter the phase spectrum so that a minimum-phase assumption could be made for the source wavelet. Spiking deconvolution can then be applied to remove the reverberating energy.

The Vibroseis (Klauder) wavelet, $w_o(t)$, is a zero-phase wavelet. It is convolved with the minimum-phase filter describing the filtering effects of the earth, $e_m(t)$, and the zero-phase reflection coefficient series, $r_o(t)$, yielding a seismic trace, $s(t)$, with mixed-phase properties.

$$s(t) = w_o(t) * e_m(t) * r_o(t)$$

For the application of spiking deconvolution, a minimum-phase equivalant must be found for the zero-phase Vibroseis wavelet. The following is a description of Ristow and Jurczyk's techniques for a finding the minimum-phase filter operator which will alter the phase characteristics of the Vibroseis wavelet. The technique is employed by Digicon's DISCO software system, which was used to process the data in this study.

Through the use of Least-Squares filtering, a filter operator can be found which will change a seismic wavelet into any desired

shape. For minimum-phase filtering, the output time series that is desired is a minimum-phase wavelet with the same amplitude spectrum of the initial zero-phase wavelet.

The problem that arises is that there is no easily obtained minimum-phase equivalent for the band-limited zero-phase wavelet. However, one can find a filter operator, using Least-Squares filtering, which has approximately the same band-pass properties as the zero-phase wavelet.

The autocorrelation function (ACF) of recorded seismic trace is used as the input for Least-Squares filtering. The desired output is a filter operator, which when convolved with the the ACF of the seismic trace will result in a spiked wavelet. A spiked wavelet is one which has coefficients of unity at t=0 and zeroes for all other times. An assumption made is that the input to Least-Squares filtering must be minimum-phase.

The ACF of the input time series, is represented in the frequency domain as:

$$ACF[s(\omega)] = A(\omega)^2 \, e^{i\phi(\omega)}$$

The filter operator determined through Least-Squares is called an inverse spiking filter, and can be represented in the frequency domain as:

$$f(\omega) = A(\omega)^{-2} \, e^{-i\phi(\omega)}$$

One can see that the inverse spike filter, $f(\omega)$, is simply the inverse of the input frequency spectrum.

After the inverse spike filter is determined by Least-Squares, it is then convolved twice with the initial zero-phase wavelet, $w_o(t)$, obtained from the autocorrelation of the recorded sweep:

$$w_o(t) \equiv A(\omega)_s = |A(\omega)|$$

where the subscript s signifies the sweep trace.

Convolving the inverse spike filter, f(t), twice with the zero-phase wavelet, $w_o(t)$, yields:

$$F(\omega) \equiv w_o(t) * w_o(t) * f(t)$$

$$F(\omega) \equiv |A(\omega)|\ |A(\omega)|\ [A(\omega)]^{-2}\ e^{-i\phi(\omega)}$$

where the result of this convolution (which is equivalent to multiplication in the frequency domain) is a phase filter operator, $F(\omega)$, with a white spectrum and a phase spectrum which is shifted 180°:

$$F(\omega) = e^{-i\phi(\omega)}$$

The phase filter operator is then time reversed to phase shift the operator 180°. Now the phase filter operator is a minimum-phase filter with a white spectrum:

$$F(\omega) = e^{i\phi(\omega)}$$

Convolving the filter operator, $F(\omega)$ with the zero-phase wavelet yields:

$$w_m(t) \equiv w_o(\omega) \cdot F(\omega) \equiv |A(\omega)|\ e^{i\phi(\omega)}$$

We now have the desired wavelet, $w_m(t)$, with the desired properties; it is a minimum-phase wavelet with the same band-limited characteristics of the initial zero-phase wavelet.

When the minimum-phase filter operator is convolved with the data trace, s(t),:

$$s(t) = w_o(t) * F(t) * r_o(t) * e_m(t)$$

$$s(t) = w_m(t) * r_o(t) * e_m(t)$$

The resulting seismic trace, s(t), now has the necessary phase characteristics to allow spike deconvolution to be applied.

For all cases which it was used, minimum-phase filtering/spike deconvolution yielded superior results to gapped predictive deconvolution. Multiple problems were noted on all SH-wave lines acquired over carbonates; however, only Line SH1 exhibited reverberations. Minimum phase filtering/spike deconvolution was used on all lines with satisfactory results. An additional discussion of this technique can be found in Gibson and Larner, (1984).

APPENDIX C

Residual Statics Analysis

Erickson et al., (1968) first discussed the importance of residual statics analysis for SH-wave data due to the longer time spent in the weathered zone and their sensitivity to lateral variations in velocity and density within this layer. Because of the slower speeds of shear-waves, random variations in the physical characteristics of geologic units, which are too small to affect P-waves, can cause relatively large time delays for SH-waves.

Preliminary processing of the SH-wave data acquired by the VTVC suggested that small time delays (less than 20 ms) had been applied to the data. This was determined while using a normal processing sequence for residual statics analysis.

Local inhomogeneities within the rock units might induce time delays which are different for different raypaths for a single recorded trace (Figure 24). The sequence of data processing using normal residual statics analysis will not remove these time variant effects.

For residual statics analysis, a time window is chosen on the record section over which autocorrelations of the traces are calculated to determine any minor variations in static shifts between adjacent traces. The window is typically chosen at a time window with high signal-to-noise ratio and at a depth where normal moveout is a

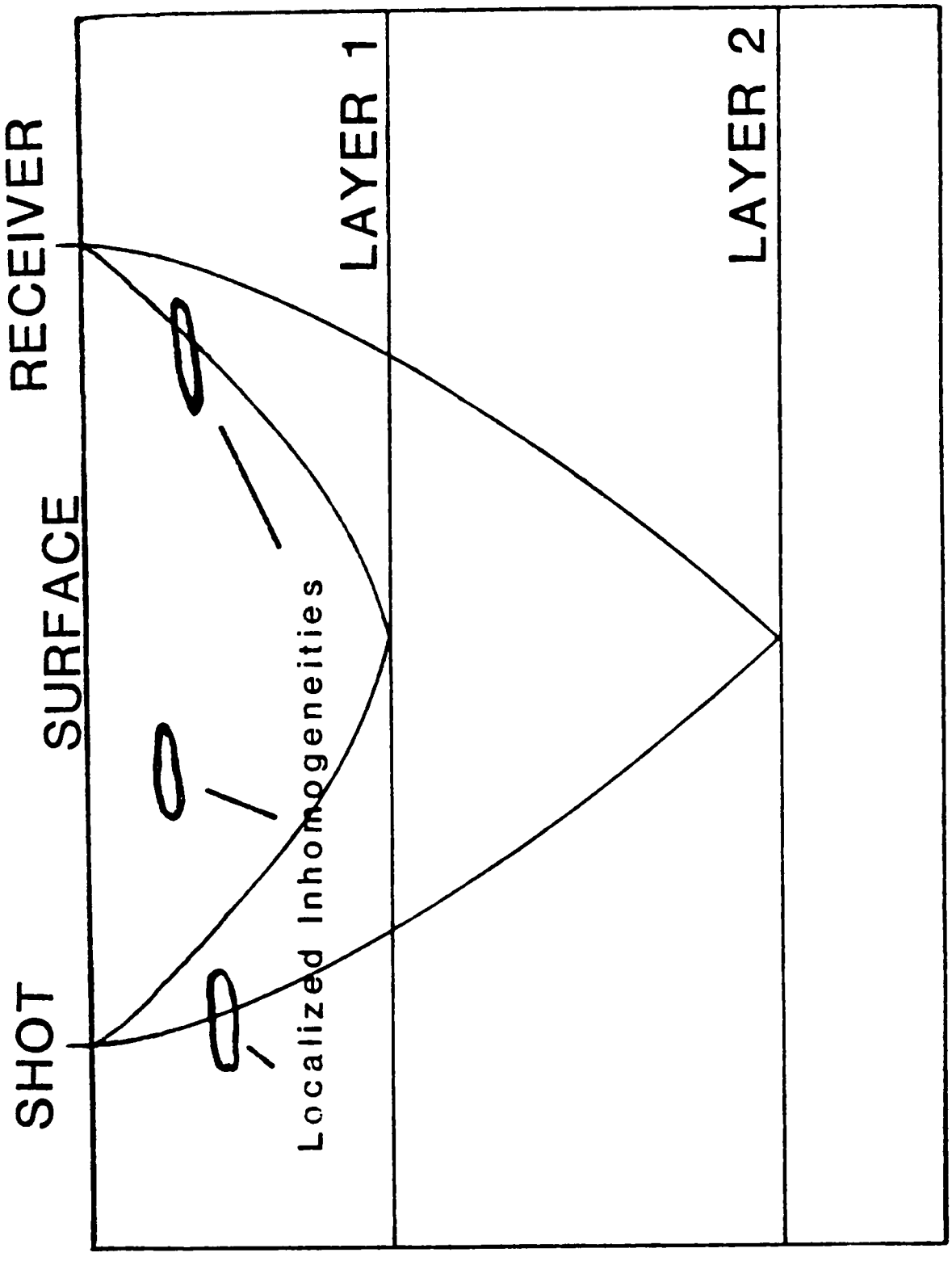

Figure 24. Local inhomogeneities within layers leading to time-variant shifts.

minimum. All of these considerations are to reduce possible errors in velocity analysis.

For the SH-wave data, a window was first chosen at a depth of 2.6-2.8 s two-way travel-time. After residual statics were applied, it was noted that the reflections at earlier travel-times degenerated. New velocities were chosen but the outcome was similar. Residual statics were then calculated for the time window at 1.4-1.8 s. The results were similar in that the reflections at 2.6-2.8 s became less coherent. New velocities were calculated again, but the results were similar. At this point it appeared that time variant shifts had been applied to the data. Similar problems have been found in areas of the Gulf Coast of the southern United States where near surface gas pockets have induced similar time shifts to data traces (J. Stubbs, personal comm., 1984).

To overcome time-variant shifts, residual statics were calculated over different time windows along the line. An approximate velocity function was chosen from that portion of the line that appeared to be least affected by statics. This velocity function was used throughout the residual statics analysis. For data processing of the SH-wave lines, two high signal-to-noise ratio time windows were chosen, centered at 1.4-1.8 and 2.6-2.8 s. Residual statics were calculated independently for each of the two time windows each with a time width of 1 000 ms. For residual statics analysis, the maximum allowable shift should be approximately half the predominant period of the wavelet. A maximum time shift of 30 ms was allowed during the processing. Multiple runs of residual statics were made to insure

the correct allowable shift. The output of previous residual statics was used as the input for latter analyses.

After residual statics were calculated and independently applied, the two record sections were summed. After summing, additional velocity and standard residual statics analysis were applied. In all cases, this procedure was found to be superior to standard processing techniques. This technique has been applied to all final shear record sections for this study.

Giles County Earthquake Locations

INSTRUMENTALLY LOCATED REGIONAL/LOCAL EARTHQUAKES

Lab.	-Reg.	Origin Time (UCT) Year	Mo	Dy	Hr:Mn:Sec	Hypocenter Location Lat-N	Long-W	Depth	NSTA	Location Parameters P/S	GAP	DMIN	RMS	SQD	Error Ellipse Proj. (ERH1, AZ1; ERH2; ERZ; Q)	Magnitude Mb/Ml/I
D	-GC	1959	04	23	20:58:40.2	37-23.70	80-40.92	5.0		/					(7.0,-82; 4.2; 0.0;)	3.8/ /
H	-GC	1968	03	08	05:38:15.7	37-16.86	80-46.44	7.7		/					(3.5,-47; 3.3; 5.8;)	4.1/ /
JR	-GC	1969	11	20	01:00:10.6	37-23.89	80-50.02	13.2	8	7/ 5	102	10	0.4	C:B	(3.0,+56; 2.8; 3.0;B)	4.6/ /
R	-GC	1974	05	30	21:28:35.3	37-27.42	80-32.40	5.4		/					(4.6,-57; 2.8; 5.1;)	3.7/ /5
S	-GC	1975	11	11	08:10:37.6	37-13.02	80-53.52	1.0		/					(6.3,-35; 3.6; 0.0;)	3.2/ /4
32	-GC	1978	01	28	23:13:23.4	37-13.68	80-44.80	4.5	3	3/ 3	243	11	0.1	D:D	(5.9, 34; 1.3; 3.0;C)	/ 1.6/
33	-GC	1978	05	10	04:19:09.6	37-12.80	80-49.82	26.2	3	3/ 3	268	12	0.1	C:D	(4.4, 44; 1.5; 3.0;B)	/ 0.3/
35	-GC	1978	06	01	01:33:01.0	37-17.99	80-41.98	17.3	3	3/ 3	170	9	0.2	C:C	(8.8, 41; 2.1; 9.1;C)	/-0.2/
37	-GC	1978	07	28	08:39:40.7	37-20.22	80-41.41	11.8	4	4/ 3	146	10	0.3	C:C	(4.9, 39; 2.2; 8.1;C)	/ 0.6/
38	-GC	1978	08	30	02:19:38.2	37-21.71	80-40.06	8.4	4	4/ 2	158	12	0.1	C:C	(3.1, 28; 1.0; 6.4;C)	/ 0.5/
46	-GC	1980	02	18	03:58:55.3	37-25.78	80-35.54	13.0	9	5/ 9	199	22	0.3	B:D	(1.7, 49; 1.2; 3.6;B)	/ 1.1/
58	-GC	1980	10	09	01:47:01.1	37-13.01	80-49.32	23.5	3	2/ 3	345	11	0.3	D:D	(7.2, 40; 2.3; 4.9;C)	/-0.2/
63	-GC	1980	12	02	07:47:38.2	37-25.08	80-32.25	12.2	6	5/ 5	113	25	0.3	C:C	(3.2, 51; 2.0; 7.4;C)	/ 0.4/
73	-GC	1981	11	12	06:24:14.0	37-14.10	80-44.99	9.2	5	2/ 4	223	10	0.2	C:D	(3.9,-67; 1.8;10.7;D)	/ 0.7/
88	-GC	1983	01	08	15:53:55.8	37-19.65	80-36.93	4.1	5	4/ 4	139	16	0.2	B:C	(1.9,-13; 1.2; 4.2;B)	/ 1.2/
90	-GC	1983	01	25	20:38:58.3	37-23.15	80-30.32	16.7	19	19/17	81	13	0.3	B:A	(0.9,-48; 0.6; 1.2;A)	/ 1.8/
92	-GC	1983	04	20	18:09:56.6	37-20.93	80-49.99	10.4	7	7/ 6	129	5	0.2	B:B	(1.8, 25; 0.9; 2.1;A)	/ 1.2/
93A	-GC	1983	05	12	00:23:07.0	37-11.49	80-43.88	14.3	5	3/ 5	202	15	0.2	B:D	(2.1,-29; 1.3; 4.0;B)	/-0.5/
93B	-GC	1983	05	17	02:02:47.7	37-15.27	80-44.09	6.9	7	5/ 7	132	9	0.3	C:B	(2.0,-18; 1.4; 5.2;C)	/-0.1/
97	-GC	1983	07	10	14:05:39.4	37-16.22	80-45.22	7.6	7	7/ 7	89	6	0.3	B:A	(1.2,-18; 1.2; 2.9;B)	/ 1.0/
101	-GC	1983	08	25	05:04:34.8	37-19.47	80-43.68	14.7	4	3/ 4	279	6	0.2	C:D	(3.0,+29; 1.8; 3.8;B)	/ 0.0/
104	-GC	1983	12	09	00:11:57.9	37-12.05	80-47.15	12.4	17	17/10	98	13	0.2	B:B	(0.7,-52; 0.6; 1.2;A)	/ 1.3/
110	-GC	1984	07	02	19:51:38.7	37-17.07	80-43.24	11.2	9	7/ 9	89	7	0.2	B:A	(1.1,+02; 0.9; 2.3;A)	/ 1.4/
114	-GC	1984	11	17	03:17:28.3	37-15.94	80-43.61	10.3	6	4/ 6	118	8	0.1	A:D	(0.4,+68; 0.3; 1.0;A)	/ 0.0/

The vita has been removed from the scanned document